A Dissertation for the Degree of Doctor of Philosophy

# Development of Absorbance and Fluorescence Spectrometer for Micro-Volume Nucleic Acids of Bio-Samples Using Total Internal Reflection

# 내부 전 반사를 이용한 미량 바이오 시료 측정용 흡광 및 형광 분광 광도계의 개발

August 2013


**Kang, In Sung**

**Major of Biosystems Engineering**

**Department of Biosystems & Biomaterials Science and Engineering**

**SEOUL NATIONAL UNIVERSITY**

A Dissertation for the Degree of Doctor of Philosophy

# Development of Absorbance and Fluorescence Spectrometer for Micro-Volume Nucleic Acids of Bio-Samples Using Total Internal Reflection

August 2013


**Kang, In Sung**

Major of Biosystems Engineering

Department of Biosystems & Biomaterials Science and Engineering

SEOUL NATIONAL UNIVERSITY

# Development of Absorbance and Fluorescence Spectrometer for Micro-Volume Nucleic Acids of Bio-Samples Using Total Internal Reflection

# 내부 전 반사를 이용한 미량 바이오 시료 측정용 흡광 및 형광 분광 광도계의 개발

지도 교수 조 성 인

이 논문을 공학박사 학위논문으로 제출함.

2013년 8월


서울대학교 대학원

바이오시스템·바이오소재학부 바이오시스템공학전공

강 인 성


강 인 성의 공학박사 학위 논문을 인준함.

2013년 8월

| | | |
|---|---|---|
| 위 원 장 | 노 상 하 | 인 |
| 부위원장 | 이 중 용 | 인 |
| 위 원 | 김 학 진 | 인 |
| 위 원 | 배 영 민 | 인 |
| 위 원 | 조 성 인 | 인 |

# Development of Absorbance and Fluorescence Spectrometer for Micro-Volume Nucleic Acids of Bio-Samples Using Total Internal Reflection

**Kang, In Sung**

## Abstract

The dedicated spectrophotometers for analysis of micro volume nucleic acids are widely used in molecular diagnostics of human health care, agriculture, food industry and etc. These have similar features of short path length and optical moving parts causing the low sensitivity and physical unstability. Besides, separate measurement system must be operated separately in order to measure both absorbance and fluorescence of bio-samples. It means high cost and low flexibility to general users.

The goal of this study is the development of the dedicated absorbance and fluorescence spectrometer for nucleic acids of bio-samples, which reduce the analysis time and the cost in half or less while improving quality of analysis in terms of the sensitivity, stability and flexibility.

In this study, a new concept of optics based on total internal reflection using a prism and a window was presented to overcome the disadvantages and improve performances of the existing instruments. Using this optics design, it is possible to measure both absorbance and fluorescence of the sample without changing the

optical structure. To determine the physical dimensions of the optics, Snell's law and Fresnel's law were applied. To optimize the design of optics, optical simulation was performed using TracePro 6.0 software. The maximum beam path length of sample was 2.83 mm and the minimum sample size was about 0.09$u\ell$ in simulation result.

The primary experimental device was fabricated to verify the adequacy of the optics design in terms of the path length accuracy, measurement accuracy, the volume of samples. As a result, the expected maximum path length by the design was 2.83mm and experimental path length was 2.81mm. The purity measurement results also showed that this optics design can be used in spectrophotometers as the standard deviation of purity measurements for the several instruments was 0.04. The minimum sample volume in real measurement can be reach to 0.2$u\ell$.

Using the verified optics, the prototype of spectrophotometer was developed and evaluated by measuring the Calf-Thymus DNA and PicoGreen-DNA in different concentrations in terms of sensitivity, LOD, baseline noise. From the experiments, the results of developed system and existed system were 9.5 and 5.75 in sensitivity, 0.18 $ng/ul$ and 0.42 $ng/ul$ in LOD, 0.0012 and 0.0028 in baseline noise. In fluorescence measurement, LOD for PicoGreen-DNA was 0.9 f mol.

From these results, it was shown that the goal of this study was achieved by enlarging the beam path length using the total internal reflection optics design.

However, to commercialize this system, the followings should be enhanced. The first is that the strength of material for total internal reflection should be more greater than that of this study not to be easily damaged in cleaning process. The second is that multi-plex optical fiber should be manufactured finely to focus the

light sources to the right position of the sample. Finally, several samples need to be measured in one time for fast measurement and well-plae or sample changer would be helpful for multi-sampling.

---

Keywords : Nucleic Acids, Spectrometer, Quantification, Purity, Total internal reflectance, Fluorescence, PCR

Student number : 2008-30332

# Contents

# List of Figures

# List of Tables

# I. Introduction

## 1. Background and Necessity

From the late 1980s, biotechnology has been developed rapidly and highlighted as a huge economic potential with a prospect of the international economy. It has been used in various fields such as agricultural, environmental, pharmaceutical and medical technology.

Biotechnology has been developed with the analytical chemistry which provides a useful tool for understanding chemical reactions taken place in molecular level. This technology changes or combines something in industrial processes using biological activity of living cells or enzymes. At this process, the functional unit is the microorganisms such as DNA or RNA can be obtained in bacteria, viruses or cultured cells in plants or mammals (Georgescu et al., 2002).

Since James Watson and Francis Crick suggested what is now accepted as the first correct double-helix model of DNA structure, various studies have been conducted on nucleic acids and several equipments handling the nucleic acids have also been developed at the same time (Bruns et al., 2007).

For example, RT-PCR is being widely used in diagnostics of various kinds of disease. It is based on the fast amplification of nucleic acids called polymer chain reaction. And various techniques for extracting nucleic acids have been also developed. The typical instrument for this area is a electrophoresis enables to separate the object with different levels of electrons.

The extraction of nucleic acids is inevitable substantial process in the biotechnology but it needs much time and efforts to get highly purity sample if we use general equipments and procedures. To overcome the inconveniences,

dedicated equipments such as automated extracting instrument(Agilent technology) and tool kits(nano-meter size micro-bid particles(Invitrogen) for easy extraction of nucleic acids were developed.

In research of nucleic acids, if there are some contaminants, the reliability of experimental result is not good enough even though we uses the high performance analytical instruments. So the purity of extracted nucleic acids is a very important factor and must be checked before full-scale study (Bruns et al., 2007).

Absorbance measurement in ultra violet region is commonly used in a purity checking process because nitrogen-containing bases strongly absorb the ultraviolet light. And quantum yield of fluorescence dye or quantum dot combined to the nucleic acids is also related to the reliable amplification of nucleic acids. These properties are measured by UV-Vis spectrometer and fluorescence spectrometer

UV-Vis spectrometer is used for the measurement of absorbance. It is a quite conventional and a basic instrument normally used in analytical chemistry for the qualification and quantification of various samples. It is based on the electronic energy transfer when the sample absorbs the light of specific wavelength.

There are several types of UV-Vis spectrometers. The most popular type is double beam UV-Vis spectrometer splits the beam to the reference and the sample. The technique of balancing and synchronization of a split beam is very important in this type of instrument. The other type is the single beam UV-Vis spectrometer with array detector. It has an ability of fast measurement by the technique of shift registering in a diode array detector. Normally, double beam UV-Vis spectrometers are used in scientific area and the single beam array UV-Vis spectrometers are used in routine area such as QC process needs fast

measurements. (Skoog et al., 2007)

But these conventional spectrometers are not suitable for the field of diagnostics because the amount of extracted DNA is about $50u\ell$ and the conventional instruments normally need over 20 $u\ell$ to measure absorbance of sample. In this case, if there is no additional treatment of DNA, about 40% of DNA should be consumed just in checking the purity. Therefore the sample must be diluted to be proper volume in conventional UV-Vis spectrometer and it may cause the inaccurate measurement results.

Since the NanoDrop equipped with a CCD array detector was released at 2001, the dedicated spectrometers for molecular diagnostics have been developed continuously and spreaded widely and rapidly. These instruments have common features. The first is minimum sample size is under 1 $u\ell$ which is suitable for checking the purity of low-volume nucleic acids. The second is very efficient as direct sampling on the optical fiber by micro-pipette is very convenient and optical components can be cleaned just by wiping with the dry paper.

However, in spite of many advantages of existing dedicated spectroscopic instruments, there are also several disadvantages and there is a necessity of the focussed research to overcome them.

The first is the low instrumental sensitivity caused by the short path length. Sensitivity is the ability to identify the difference of samples in low concentrations and it depends on the beam path length of sample. Generally, the concentration of extracted nucleic acids in the field of diagnostics is very low and the higher measurement sensitivity the higher diagnostics accuracy and reliability.

And the second is relatively low stability comparing conventional spectrometers caused by repetitive moving the optical fiber for fixing the micro-volume samples

because the dedicated spectrometers commonly use a pair of optical fibers to attach the samples by retention effect. After measuring the sample, one of the optical fibers should be opened to clean the sample. In this way, the optical beam path can be mis-arranged which can cause the instability of the data.

The last thing is low flexibility by using the separate systems to measure the absorbance and fluorescence of a sample. Operating separate system needs more amount of sample and it means the inefficiency and high cost. In addition, to purchase additional equipment needs high cost.

## 2. Objectives of the study

The goal of this study is the development of the dedicated absorbance and fluorescence spectrometer for nucleic acids of bio-samples, which reduce the analysis time and the cost in half or less while improving quality of analysis in terms of the sensitivity, stability and flexibility.

Specific objectives of this study are:

1) to develop a specific optical system based on total internal reflection of which geometry requires less volume of bio-samples, provides longer path length than the state-of-the-art, and affords simultaneous measurement of absorbance and fluorescence spectra to enhance the performance of spectrophotometer for micro-volume bio samples.

2) to develop the spectrophotometer by integrating the light source, optical fibers, and softwares et al.

3) and to evaluate the developed spectrophotometer in terms of the sensitivity, stability and flexibility

The main items which determine the sensitivity, stability and flexibility of the system to be developed were listed with quantitative target in Table 1. Sensitivity is related to the beam path length as the longer path length enables to get the higher absorbance. And stability is related to the limit of detection, baseline noise. The flexibility is related to the minimum sample size and ability of measuring both of absorbance and fluorescence spectra of samples. As shown in this Table, the performance of the system from this study should be improved about 2 times better than that of the NanoDrop 2000, the dedicated spectrometers which has the highest market share.

Table 1. Quantitative target of this study

| **Items** | **Target of development** | **NanoDrop 2000** |
|---|---|---|
| Minimum Sample Size | 0.2 $\mu\ell$ | 0.5 $\mu\ell$ |
| Maximum Path Length | 2.8 mm | 1mm |
| Detection Limit | 1 $ng/\mu\ell$(dsDNA) | 2 $ng/\mu\ell$ (dsDNA) |
| Baseline Noise | 0.001 AU | 0.002 AU |
| Measurement Option | Fluorescence & Absorbance | Absorbance only |

# II. Literature Review and Basic Principles

In oder to develope the dedicated simultaneous absorbance and fluorescence spectrometer for nucleic acids of bio-samples with better quality of analysis, literature on absorption and fluorescence measurement of nucleic acids and development of measurement system for Micro-Volume sample were reviewed. In the later part of this chapter, basic principles and information of the state of art related to the spectrophotometer systems were introduced.

## 1. Literature Review

### 1.1 Absorption and Fluorescence Measurement of Nucleic Acids

In absorption measurement, Zhang checked the purity of RNA using Nano Drop before analysis of RT-PCR for diagnosis of rice strip virus (RSV). The purity of extracted DNA was measured by Nano Drop and the value was over 2.0 (Zhang et al., 2008). After confirming the purity of the RNA by comparing A260nm/A230nm and A260nm/A280nm, high-purity samples were measured to diagnose four tomato viruses at the same time by RT-PCR (Mortimer-Jones et al., 2009). Zhang measured the purity of DNA in wheat and applied the samples of purity over 1.8 to RT-PCR for detection of the wheat dwarf virus (WDV) (Zhang et al., 2010). And simple, accurate, sensitive method for small RNA expression based PCR was presented (Ro et al., 2006). To define the optimum quantification for DNA, six different quantification methods was presented. The conclusion of this study was international standard DNA materials and method should be fixed for reasonable quantification (Nielsen, et al., 2006)

In fluorescence measurement, the research of quantification nucleic acids using fluorescent dye, quantum dot, green fluorescent protein (GFP) has been in progress since a fluorometric method for RNA and DNA determination using ethidium bromide (EB) dye increasing fluorescence quantum efficiency (Pecq et al., 1966). And SYBR Green II dye was used for the quantification of RNA in nanogram sensitivity as low as 0.5ng/ml (Schmidt et al., 1995). Quantitation of human DNA based on probe hybridization was performed and less than 150 pg of human DNA could easily be detected with 15 minutes exposure. (Walsh et al., 1992). GFP with microscopic imaging technique was applied to detect the transgenic of tobacco (Blumenthal et al., 1999). It was proved that SYBR Green and PicoGreen were substantially more sensitive for quantifying DNA by comparing high sensitive and rapid way to evaluate the DNA content of samples based fluorescence measurement (Rengarajan et al., 2002). Hoechst 33258 and SYBR Green II dyes were used in quantification of RNA and DNA (Morozkin et al., 2003). In these days, quantum dot as the fluorescence probe has been widely researched. Interaction between CdSe/ZnS core-shell quantum dots (QDs) and bovine serum albumin (BSA) protein was studied and this QD was very applicable to humane serum albumin (Dzagli et al., 2010). Composite polymer particles consisting of a solid poly core and a polymer shell doped with quantum dots were fabricated and used as temperature sensor, as carriers for biomolecules in biosensing employing optical detection. (Generalova et al., 2012). Recently, micro-volume sample was also measured by dedicated fluorescence spectrometer. Sandra proposed that NanoDrop fluorospectrometry can also be applied for measuring enzyme activities using fluorogenic substrates such as the proteolytic activities of the 26S proteasome (Gotze et al., 2011).

## 1.2 Development of Measurement System for Micro-Volume Sample

The research of the development of equipment for measuring the micro-sample for diagnosis has been focused to downsizing of sampling module for effective experiment. Lab-on-a-chip, protein chip. PDMS, glass, silicon were used to fabricate fluid and temperature controlled micro chip for analyzing functional small size protein (Shim, 2007). A fully integrated biochip device consists of micro-fluidic mixers, valves, pumps, channels, heaters, and DNA micro-array sensor was developed to perform DNA analysis of complex biological sample solutions (Liu et al., 2004). And field effective transistor (FET)-type DNA charge sensor was fabricated on 0.5um standard complementary metal oxide semiconductor (CMOS) technology of detecting the deoxyribonucleic acid probe's immobilization (Kim et al., 2004). An experimental approach was presented to conducting fast capillary electrophoresis-mass spectroscopy measurements of very small samples in nanoliter range. In this research, the concept of capillary batch injection was used to increase injection efficiency. (Grundmann et al., 2012).

Total internal reflection fluorescence microscopy has been researched in cell biology. The prism based on TIR in an inverted microscope was presented as Fig. 1 (Axelrod, 2001). In this report, the buffer filled sample chamber consists of a lower bare glass cover slip, a spacer ring and the cell cover slip inverted for the cells to be faced down. And several recent developments in total internal reflection fluorescence methodology from other fields are likely to find proper application in cellular biophysics (Thompson et al., 2005). And the interaction and adsorption of bovine serum albumin (BSA) and meso-tetrakis (4-sulfonatophenyl) porphyrin (TPPS) at toluene–water interface were studied successfully by the coupling technique of total internal reflection synchronous

fluorescence (Marras et al., 2008). Kang designed the equipment for measuring fluorescence information of bio-chip using the total internal reflecting light source (Kang et al., 2007). In this design, wide field fluorescence measurement was implemented by new concept of illumination.

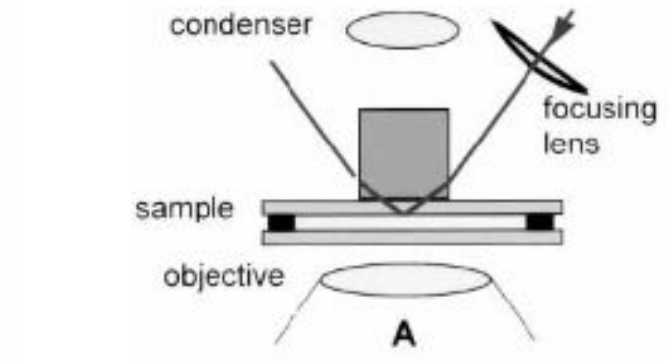


Fig. 1 Principle of fluorescence light intensity enhancement via total internal reflection in microscope (Axelrod, 2001)

# 2. Basic Principles

## 2.1 Spectroscopic Properties of Nucleic Acids

### 2.1.1 The features of absorption in UV region

Structures of nitrogenous bases of nucleic acids including DNA, RNA, nucleotide, nucleoside and other nitrogen-containing bases are shown in Fig. 3. The nitrogen-containing nucleotide of these bio-materials strongly absorb the ultraviolet light and show maximum absorption peak at 260 nm wavelength as shown in Fig. 2. On the other hand the maximum peak wavelength of protein is 280nm and the purity of nucleic acid can determined by calculating $A_{260}/A_{280}$. (Boyer et al., 2000).

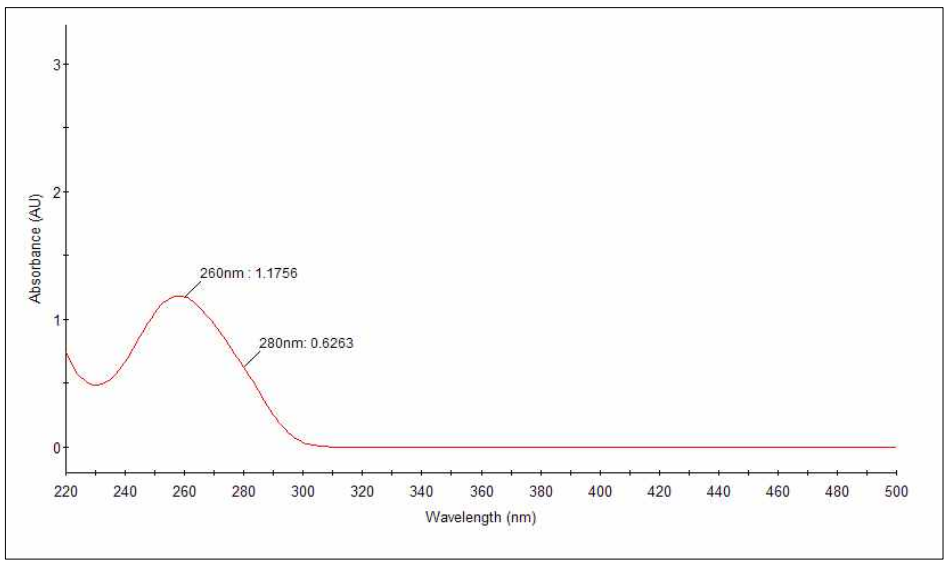


Fig. 2 A typical absorption spectrum of DNA

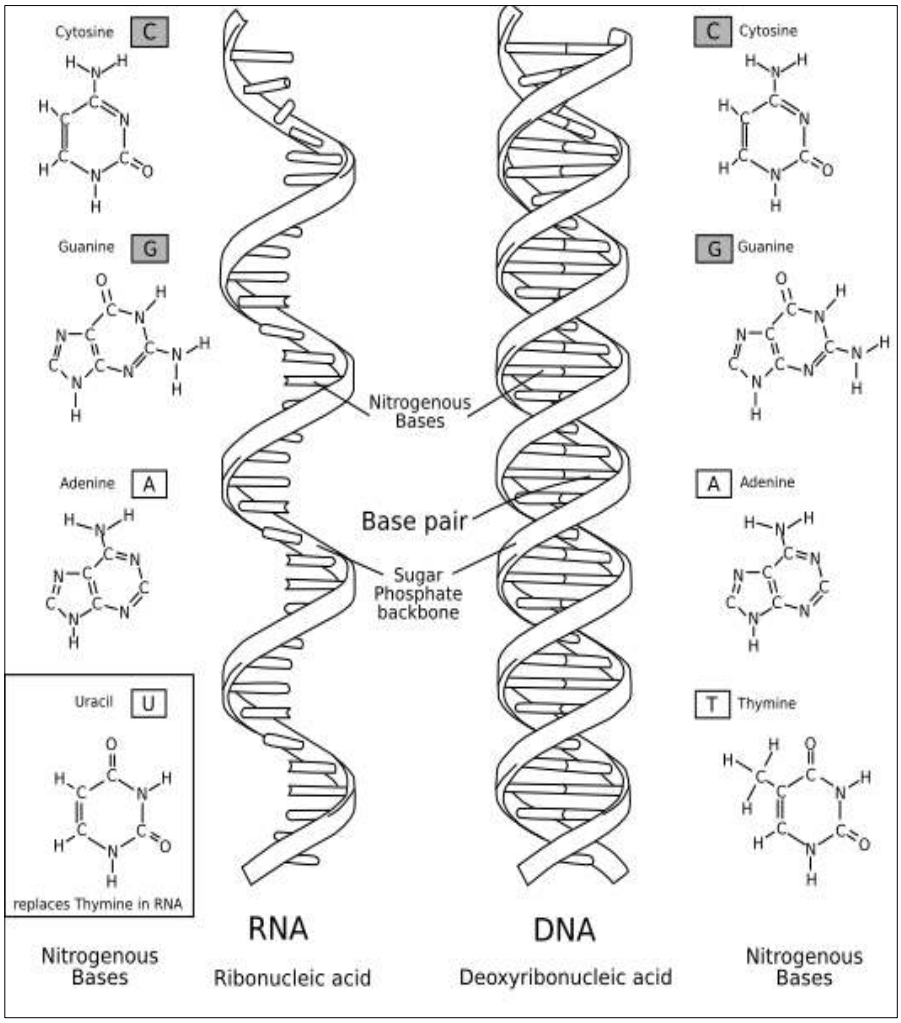


Fig. 3 Structure of nitrogenous bases of nucleic acids

### 2.1.2 Quantification of Nucleic Acids

As shown in Fig. 2, nucleic acid has a maximum absorbance at 260 nm, and high concentrated nucleic acid absorbed more light.

Using the Beer-Lambert Law, it is possible to relate the amount of light absorbed to the concentration of the absorbing molecule. At wavelength of 260

nm, the average extinction coefficient is 0.02 for double-stranded DNA, 0.027 for single-stranded DNA and 0.025 for single-stranded RNA. Thus, an absorbance of 1 corresponds to a concentration of 50 μg/ml for double-stranded DNA and of 40 ug/ml for RNA. (Bruns et al., 2007). In this way, the quantification of nucleic acids follows the formula 1 and 2.

$$[RNA]\,ug/ml = A_{260} \times 40 \times D \quad \text{----------(1)}$$

$$[dsDNA]\,ug/ml = A_{260} \times 50 \times D \quad \text{----------(2)}$$

where,

$A_{260}$ : absorbance at 260nm

$D$ : dilution factor

Quantification of DNA in solution is a common application in all areas of molecular biology research. Checking the amount of DNA is the first step for DNA sequencing and evaluation of purity of DNA in recombination protein products.

Recently, fluorescence measurement of DNA is widely applied to several biological sensing technologies such as RT-PCR, micro-array as it's sensitivity is about 1,000 times better than that of absorbance.

### 2.1.3 Purity of Nucleic Acids

DNA, and other proteins shows different absorbances at different wavelength as shown in Fig. 4. The purity of nucleic acids is defined by the ratio of absorbances at 260 nm and that of 280 nm (Held, 2001). For DNA analysis,

purity should be over 1.8 and it should be over 2.0 for RNA analysis. If the ratio is lower than the values of each case, it means the presence of protein, phenol or other contaminants that absorb strongly at or near 280nm. The ratio of $A_{260}/A_{230}$ is used as a secondary measure of nucleic acid purity if there is an absorption at 230nm such as Guanidine HCL used for DNA isolations. as Fig. 5.

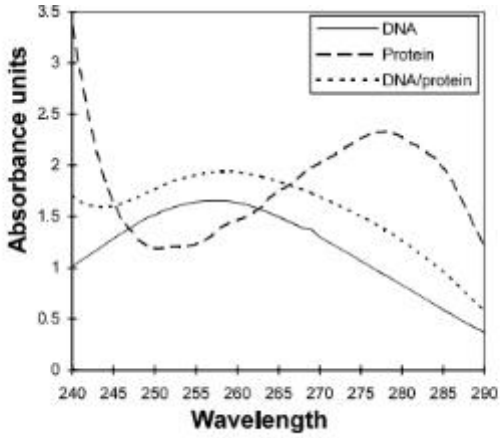


Fig. 4. The typical absorption spectra of DNA and Protein (Held, 2001)

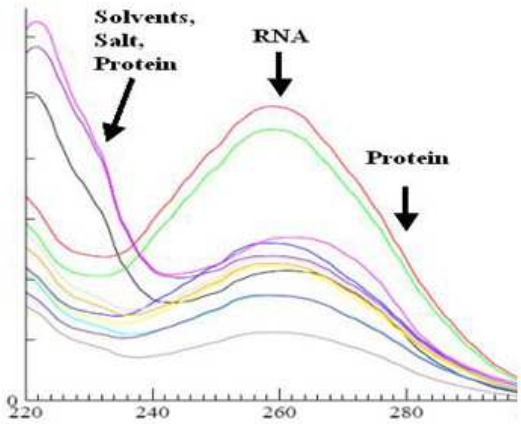


Fig. 5. Absorption measurements of nucleic acids to determine purity ratio by A260/A230 (FlyChip)

### 2.1.4 Fluorescence Spectrum of Nucleic Acids

Nucleic acid binding fluorescent dyes are about 1,000 times more sensitive than absorbance measurements. Cyanine dyes such as SYBR Green1 have no fluorescent light before combining to the nucleic acid and it can be used to visualize the amplification of nucleic acids. Several dyes that are specific for nucleic acids and protein are listed in Table 2. Generally, fluorescence dyes are not affected by the presence of common contaminates such as protein and carbohydrate molecules as fluorescent dyes react to the specific wavelength (Marras et al., 2008)

Table 2. Various fluorescence dyes for quantification of DNA in solution (Pheonix Research Products, 2011)

| DNA Quantification | Excitation Wavelength | Emission Wavelength |
|---|---|---|
| DAPI | 360nm | 465nm |
| Hoechst 33258 | 360nm | 465nm |
| PicoGreen | 485nm | 535nm |
| RiboGreen | 485nm | 535nm |
| OliGreen | 485nm | 535nm |
| **Protein Quantification** | **Excitation Wavelength** | **Emission Wavelength** |
| cyanine dyes (e.g. YO-YO-1) | varies | varies |
| ethidium bromide | 520nm | 605nm |
| SybrGreen I | 485nm | 535nm |
| Quant-iT Protein Assay | 470nm | 600nm |

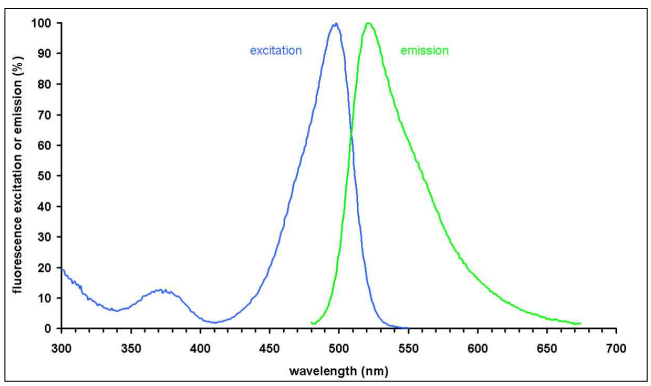


Fig. 6 Fluorescent excitation and emission spectra of DNA binding to the SYBR Green I

To develop a quantum dot or fluorescent dye, quantum yield of the material is the important factor and can be defined by formula 3 (Lakowicz, 1999). On this formula, $OD$ can be measured by absorption spectrometer and fluorescent intensity $I$ can be measured by fluorescence spectroscopy.

From this reason, if the absorbance and fluorescence could be measured in one system, it would be efficient to determine the quantum yield of the material.

$$Q = Q_R \frac{I}{I_R} \frac{OD_R}{OD} \frac{n^2}{n_R^2} \text{ ----------(3)}$$

where,

$Q$ : quantum yield,

$I$ : fluorescence intensity

$OD$ : optical density

$n$ : refractive index

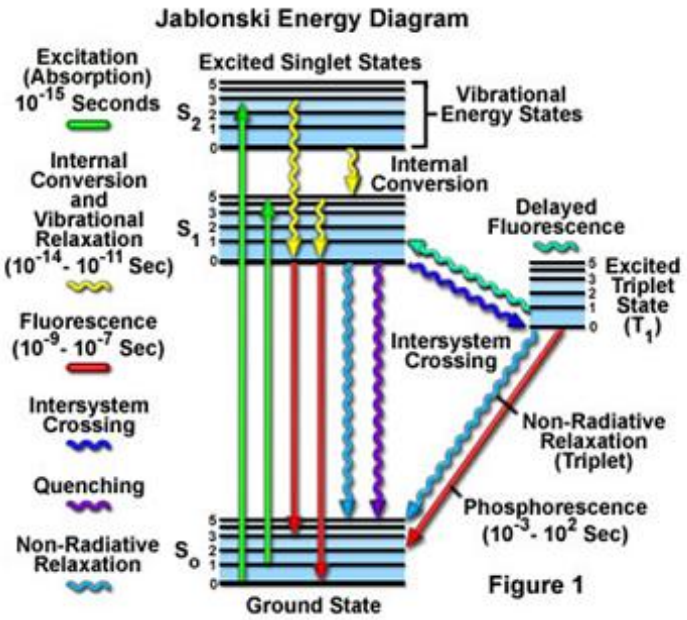


Fig. 7 Jablonski energy diagram on light absorption and emission in the molecular energy transfer (Olympus)

## 2.2 Dedicated Spectrometer for Micro-Volume Nucleic Acids

The amount of nucleic acid extracted in elution buffer is 50 $u\ell$ ~100 $u\ell$ as shown in Fig. 11. DNA concentration in elution buffer is very low and the most part of extracted DNA must be amplified by PCR method for the diagnosis of disease. Therefore, very small part of extracted DNA should be used for measuring purity and micro-volume cuvettes which are used for sampling small samples as Fig. 8.

In conventional UV-Vis spectrometer, these small samples must be diluted even though the micro-volume cuvettes is used as it needs over 20$u\ell$ for reliable measurement results. If there is no dilution, about 20~40% of extracted DNA should be consumed for just checking the purity. Repetitive dilution needs much time and may be the source of inaccuracy in diagnostics as there are lots of samples to be measured. Besides, micro volume cells have very narrow inlet, which is not easy to be cleaned.

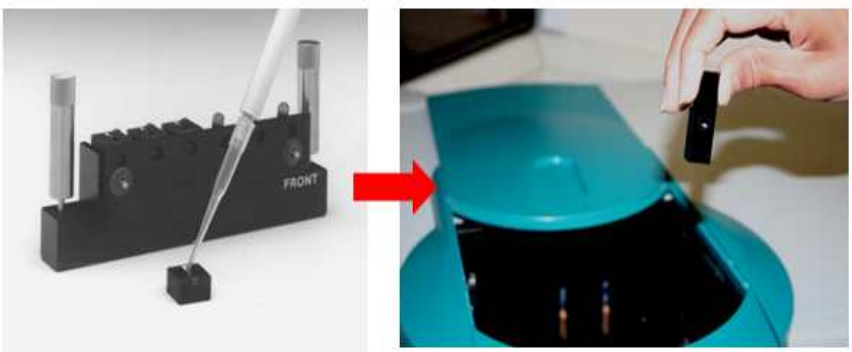


Fig. 8 Conventional UV-Vis Spectrometer with micro-volume cell for measuring micro-volume sample

From these reasons, the technology of direct measurement of small nucleic acids without pre-treatment became necessary and several instruments such as NanoDrop (Thermo Fisher Scientific) and Nano-Vue (GE Healthcare) have been launched.

The basic structure of these devices consists of two optical fibers as Fig.9. A sample is placed between two optical fibers and is fixed by its own surface tension called 'Retention'. Two optical fibers are arranged to input the light to the sample and to transfer the sample transmitted light to the spectrograph. The beam path length can be adjusted from 0.1 to 1 mm.

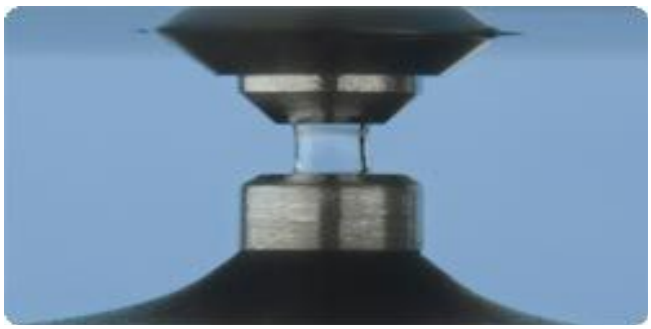

Fig. 9 View of micro-volume sample retained between two ends of the optical fibers (NanoDrop 2000)

The advantages of these devices are direct sampling on the pedestal without additional cuvette and convenience in cleaning the optics. The end surface of the optical fiber is easily cleaned as shown in Fig. 10.

Fig. 10 Cleaning and sample placing processes for the quantification of nucleic acids using the dedicated spectrophotometer (NanoDrop 2000)

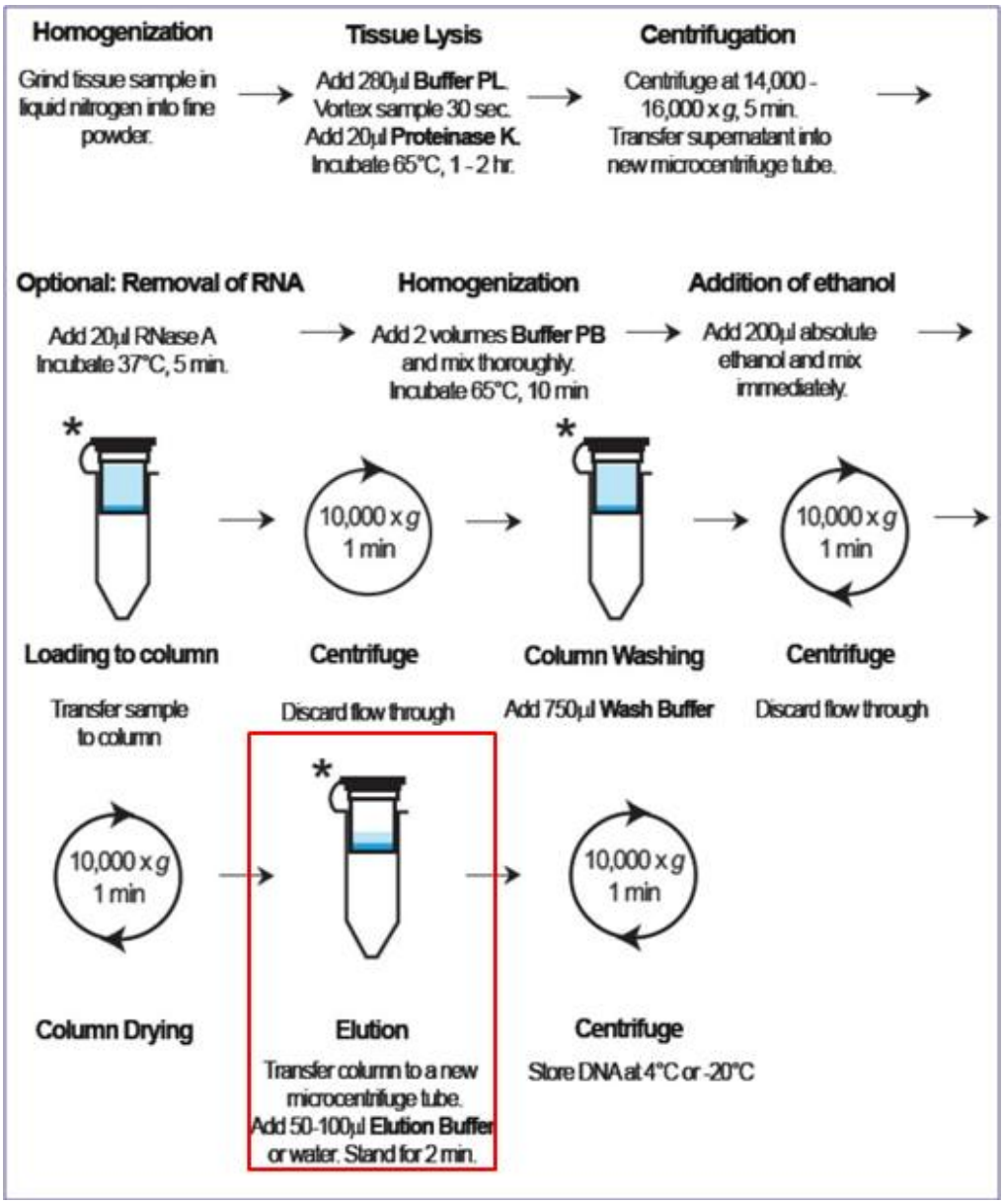


Fig. 11 Procedure of DNA extraction using GF-1 plant DNA isolation kit produced by GeneOn

## 2.3 Optics theory

### 2.3.1 Beer-Lambert's Law

Beer–Lambert's law, also known as Beer's law or the Lambert–Beer law or the Beer–Lambert–Bouguer law (named after August Beer, Johann Heinrich Lambert, and Pierre Bouguer) relates the absorption of light to the properties of the material (Douglas A. et al., 2007).

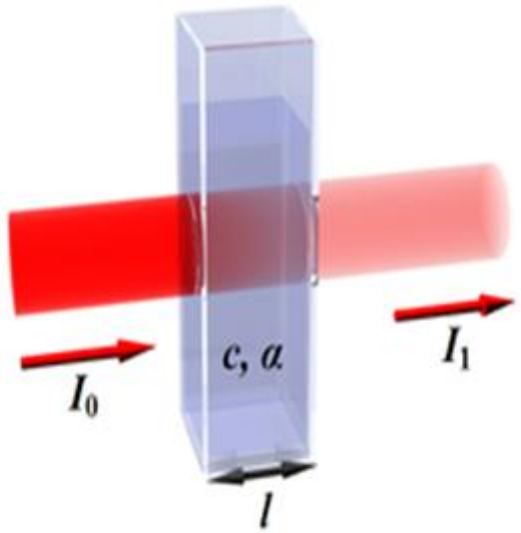


Fig. 12 Variables employed in Lambert's law

Lambert's law is credited with the first mathematical formula of this effect, although is now appeared that Bouguer first stated it in 1729. The mathematical expression is

$$T = I_1/Io = e^{-ab} \quad \text{----------(4)}$$

Where,

$T$ : transmittance of sample

$Io$ : the incident intensity

$I$ : the transmitted intensity

$a$ : regression coefficient

$l$ : the path length

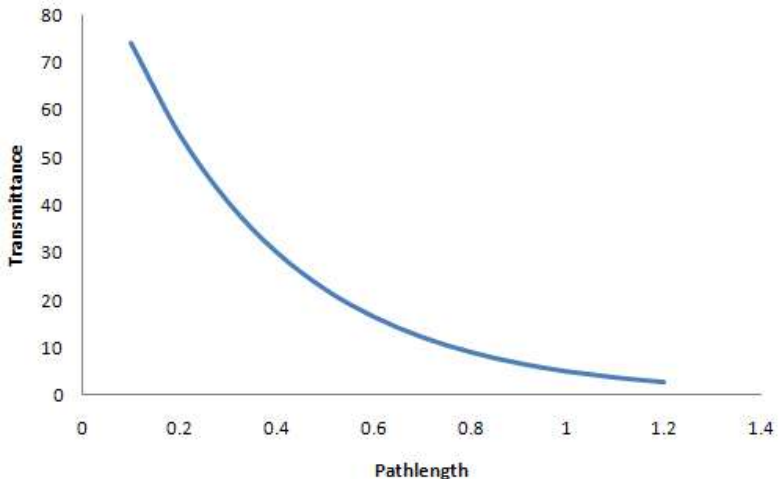


Fig. 13 Exponential relationship of transmittance to optical beam path length

Beer's law is identical to Bouguer's law except that it is stated in terms of concentration. The amount of light absorbed is proportional to the number of absorbing molecules through which the light passes.

Combining the two laws gives the Beer-Lambert-Bouguer law as follow formula.

$$T = I_1/Io = e^{-klc} \quad \text{----------(5)}$$

where,

$k$ : molar absorptivity

$c$ : sample concentration

This formula can be transformed into a linear expression by taking the logarithm and is usually expressed in the decadic form as formula 6.

$$A = -\log T = -\log(I_1/Io) = \log(Io/I_1) = \epsilon lc \quad \text{----------(6)}$$

where,

$\epsilon$ : molar absorptivity or molar extinction coefficient

The extinction coefficient is a characteristic of a given substance under precisely defined set of conditions, such as wavelength, solvent, and temperature. In practice, the measured extinction coefficient also depends partially on the characteristics of the instrument. For these reasons, predetermined values for the extinction coefficient usually are not used for quantitative analysis. Instead, a calibration or working curve for the substance to be analyzed is constructed using one or more standard solutions with known concentrations.

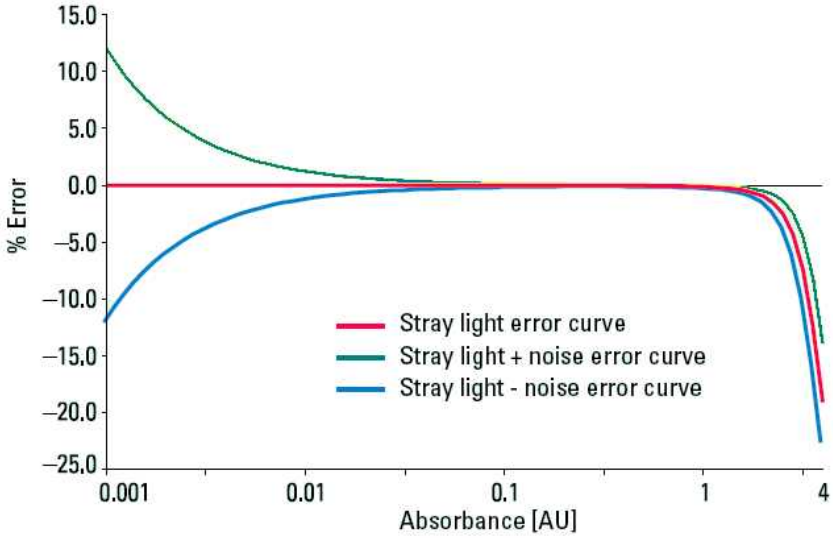


Fig. 14 Absorbance measurement errors due to stray light and noise at various absorbance (Agilent Technologies, 2000)

Ideally, absorbance and concentration has a linear relationship for whole range of absorbance. But actually, there are several factors cause the error of the results. For the low or high absorbance samples, the error easily can be increased by stray light and electrical noise of detection devices as Fig. 14. To minimize the absorbance error, beam path length should be adjusted to ensure absorbance level from 0.1 to 1 because absorbance is also related to the beam path length and concentration. Fig. 15 shows typical cuvettes with various path length for conventional UV-Vis spectrometers.

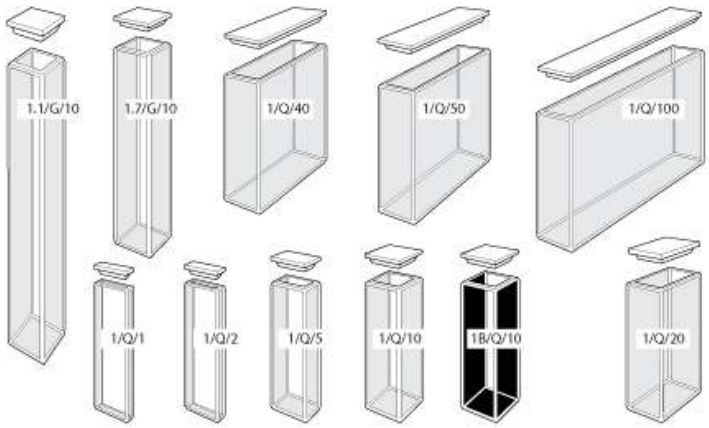


Fig. 15 Various cuvettes with different path lengths for conventional spectrophotometer

### 2.3.2 Snell's Law

Whenever the light is incident on the boundary separating two different media, part of the ray is reflected back into the first medium and the remainder is refracted as it enters the second medium as Fig. 16. The directions taken by these rays can be described by two well-established laws of nature.

According to the simplest of these laws, the angle at which the incident ray strikes the interface *MM′* is exactly equal to the angle the reflected ray makes with the same interface. Instead of measuring the angle of incident and the angle of reflection from the interface *MM′*, it is customary to measure both from a common line perpendicular to this surface. This line *NN′* in the diagram is called the normal. As the angle of incident ø increases, the angle of reflection also increases by exactly same amount, so that for all angles of incidence. (Jenkins et al., 2001).

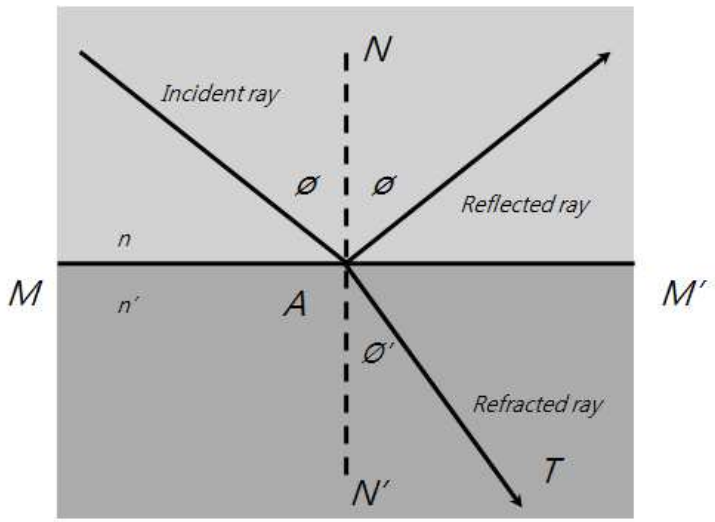


Fig. 16 Refracted and reflected light on the layer of different media

The second law is concerned with the incident and refracted rays of light, and states that the sine of the angle of incidence and the sine of the angle of refraction bear a constant ratio one to the other, for all angles of incidence :

$$\frac{\sin \Phi}{\sin \Phi'} = \text{const} \quad \text{----------(7)}$$

where,

$\Phi$ : incident angle

$\Phi'$ : refracted angle

And the refracted ray also lies in the plane of incidence and on the opposite side of the normal. This relationship, experimentally established by Snell is known as Snell's law. In addition the constant is found to have exactly the ratio of the refractive indices of the two media $n$ and $n'$. Hence we can write

$$\frac{\sin \Phi}{\sin \Phi'} = \frac{n'}{n} \quad \text{----------(8)}$$

where,

$n'$ : refractive index of second media

$n$ : refractive index of first media

### 2.3.3 Fresnel's Law

The essential features of reflection from a single surface are briefly described as follows. At normal incidence about 4 percent of the intensity of a beam of

unpolarized visible light is reflected, and the other 96 percent is transmitted. At other angles of incidence the reflecting power increases with angle, at first slowly and the more rapidly until at $90^{o}$, that is, grazing incidence, all the light is reflected.

And there is one angle of incidence for which the reflected light is completely plane-polarized with its electric vector perpendicular to the plane of incidence. At angles different from this the reflected light is only partially polarized. The relations in this case are most easily described in terms of the reflection of the two plane-polarized components of the incident unpolarized light, the vibrations of which are, respectively, parallel and perpendicular to the plane of incidence

In the laboratory this is usually done by examining the reflected light that passes through a polarizer as Fig. 17.

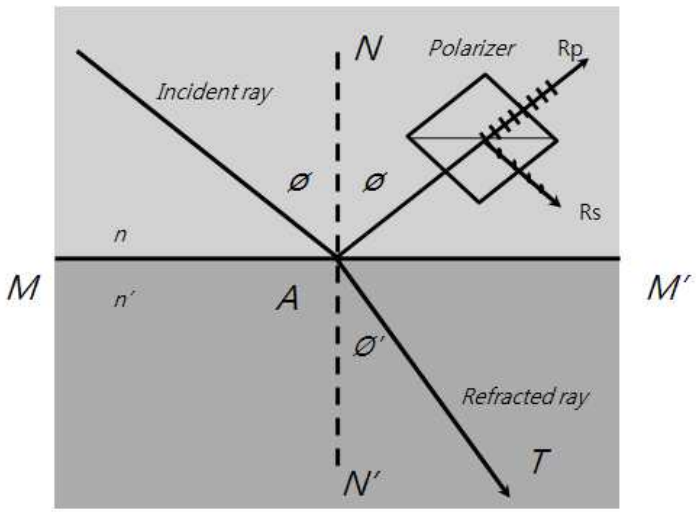


Fig. 17 Reflected light into it's two plane-polarized components

If the polarizer is oriented with its principal section parallel to the plane of incidence, the p vibrations, i.e., the vibrations parallel to the plane of incidence, can be measured. Rotation of the polarizer through 90° then allows the s vibrations perpendicular to the plane of incidence to be measured. The results of such an experiment when plotted against the angle of incidence ø are represented by the two solid curves shown in Fig. 18. The curves are represented very accurately by theoretical formulas which were first derived by Fresnel from the elastic-solid theory and are known as Fresnel's laws of reflection. The laws can be written as formula 9, 10 (Jenkins et al., 2001).

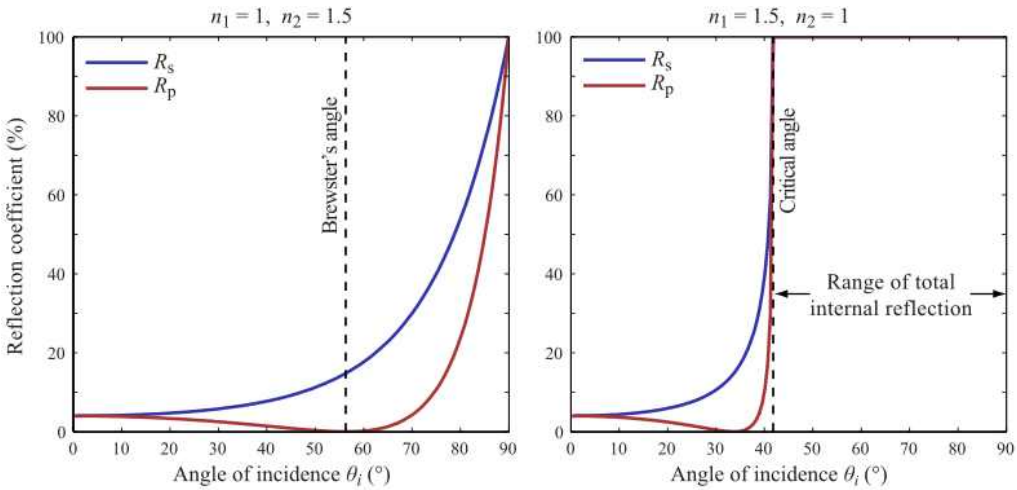


Fig. 18 Reflectance plot of different phase of light

$$Rs = \left| \frac{ncos\phi - n'\cos\phi'}{ncos\phi + n'\cos\phi'} \right|^2 = \left| \frac{ncos\phi - n'\sqrt{1-(\frac{n}{n'}sin\phi)^2}}{ncos\phi + n'\sqrt{1-(\frac{n}{n'}sin\phi)^2}} \right|^2 \qquad \text{-------(9)}$$

$$Rp = \left| \frac{n\cos\phi' - n'\cos\phi}{n\cos\phi' + n'\cos\phi} \right|^2 = \left| \frac{n\sqrt{1-(\frac{n}{n'}\sin\phi)^2} - n'\cos\phi}{n\sqrt{1-(\frac{n}{n'}\sin\phi)^2} + n'\cos\phi} \right|^2 \quad \text{------(10)}$$

where,

$\Phi$ : incident angle

$\Phi'$ : refracted angle

$n'$ : refractive index of second media

$n$ : refractive index of first media

## 2.4 Optical Components

### 2.4.1 Diffraction Gratings

A grating consists of a series of equally spaced parallel grooves made on the surface of a suitable material such as polished glass or copper and over coated with a reflective material. Two types of gratings are available. Ruled gratings are made by ruling parallel grooves using precision ruling engine with diamond tool whiles holographic gratings are made using interferometer technique to produce interference fringes on a material coated with photo resist followed by developing.

In view of the shape, reflective diffraction grating can be classified into two types. The first is plane grating and the other is concave grating and both grating follow formula 11 (Loewen et al., 1997).

The distance between the adjacent grooves or fringes and the angle the grooves form with respect to the substrate surface help to determine the dispersion and efficiency of a grating. In order to maximize the performance of a grating, energy

must be concentrated into one of the orders (except the zero order) as energy distribution depends on the groove shape. The principle is to rule the grating so that the reflecting groove is tilted with respect to the grating surface. For holographic gratings the profile of the sinusoidal shape is important.

Transmission gratings are made on polished glass surfaces deposited with index matched epoxy resin. Ruled and holographic transmission gratings are commonly used for laser beam division and multiple laser line separation in wide spectral region in the visible region. The transmitted beam is diffracted into multiple orders. By optimizing grating parameters such as materials, coating and groove profile various gratings can be produced offering different dispersion, polarization and power distributions.

The general grating formula which enables selection to separate polychromatic radiation into its constituent wavelength is usually written as:

$$n\lambda = d(\sin\alpha \pm \sin\beta_n) \quad \text{----------(11)}$$

where,

$n$ : order number of diffraction,

$\lambda$ : wavelength of light dispersed

$d$ : distance between successive groves or fringes

$\alpha$ : angle of incidence measured from the grating normal

$\beta_n$ : angle of diffraction of the nth order measured from the grating normal

$\Theta$ : blazed angle

In the littrow configuration ($\lambda = \beta_n$), the grating formula reduces to $n\lambda = 2d$

$sin\alpha$ and for transmission gratings at normal incidence, the grating formula becomes $n\lambda = d\ sin\beta n$ (Loewen et al., 1997).

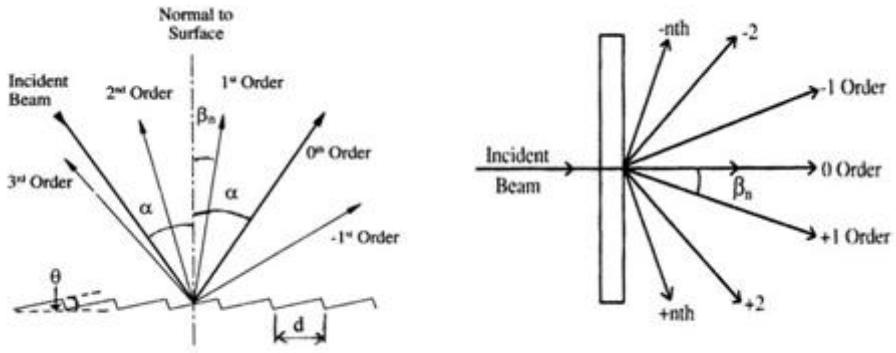


Fig. 19 Dispersed light on the reflectance grating and transmission grating

As seen in Fig. 19, there are several orders of diffracted light and only one order light normally is used for measurement of spectrum. For example, the 200nm wavelength light can be over-layed with those of 400nm, 600nm, 800nm and the second order light of 200nm will affect the data on other regions. So this must be blocked by optical filters such as long pass filter or interference filter. This is called order sorting filter and it must be attached on the sensor in spectrometer.

Fig. 20 shows typical spectrographs with the plane reflection grating and concave grating. Plane grating is easy to be produced with low cost for fabricating the spectrograph. However additional optical components should be used to collimate and focus the light. To enhance the performance in the UV region, concave grating can be used as it does not need any reflectors which can cause the stray light and scattering inside of spectrograph.

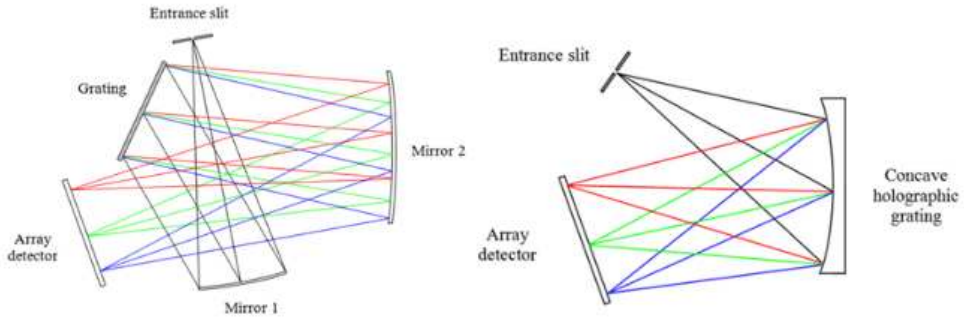


Fig. 20 Typical spectrographs with plane grating and concave grating

### 2.4.2 Optical Fiber

To transfer the light to the position on which the optical components can not be mounted, optical fibers can be used as the beam pathway could be easily changed without reflector and it can be mounted in narrow spaces indeed.

The optical fiber is comprised of a light-carrying core (higher refractive index) surrounded by a cladding (lower refractive index). This construction traps the light in the core by the principle of total internal reflection. Since the fiber core has a higher refractive index, the light in the core is totally reflected at the boundary of the cladding for all light that strikes at greater than the critical angle. The core and cladding are usually fused silica glass covered by a plastic coating, called 'buffer' and it protects the glass fiber from physical damage and moisture (Crisp et al., 2005)

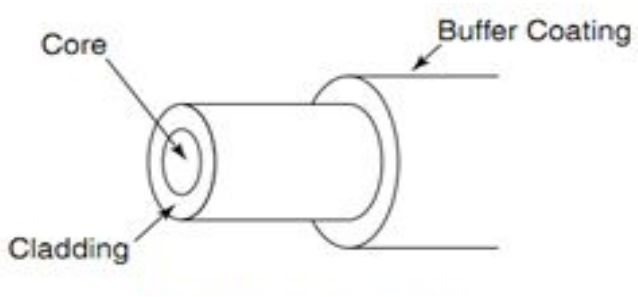


Fig. 21 Typical structure of optical fiber

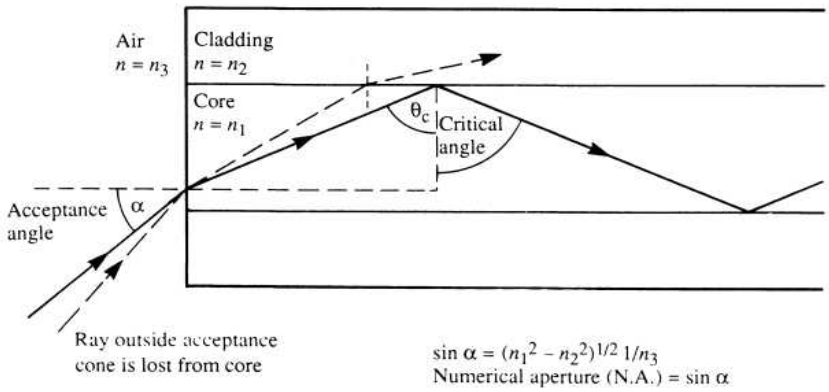


Fig. 22 Light pass inside of the optical fiber

Fig. 22 shows that a ray that meets the first core-cladding interface at the critical angle. This ray incidents at the fiber core at an incident angle of $\alpha$, this incident angle $\alpha$ is defined as the acceptance angle of the fiber. Any light rays incident at the fiber core with an angle greater than $\alpha$ will not be refracted sufficiently to undergo 'Total Internal Reflection' at the core-cladding interface, and therefore, although they enter the core, they will not be accepted into the fiber for onward transmission. Acceptance angle is measured in air out of the fiber. The acceptance angle normally is regarded as numerical aperture (NA) (Crisp et al., 2005)

$$NA = n_{air} \sin\alpha = \sqrt{n_1^2 - n_2^2} \quad \text{----------(12)}$$

where,

$NA$ : numerical apeture

$n_{air}$ : refractive index of air

$n_1$ : refractive index of core

$n_2$ : refractive index of cladding

### 2.4.3 Light Sources

Ultraviolet (UV) and visible radiation take only a small part of the electromagnetic spectrum, which includes such other forms of radiation as radio, IR, cosmic, and Xrays. The energy related with electromagnetic radiation is defined by the following formulas :

$$E = h\nu \quad \text{----------(13)}$$

where,

$E$ : energy of radiation,

$h$ : Plank's constant ($6.62 \times 10^{-34}$)

$\nu$ : frequency

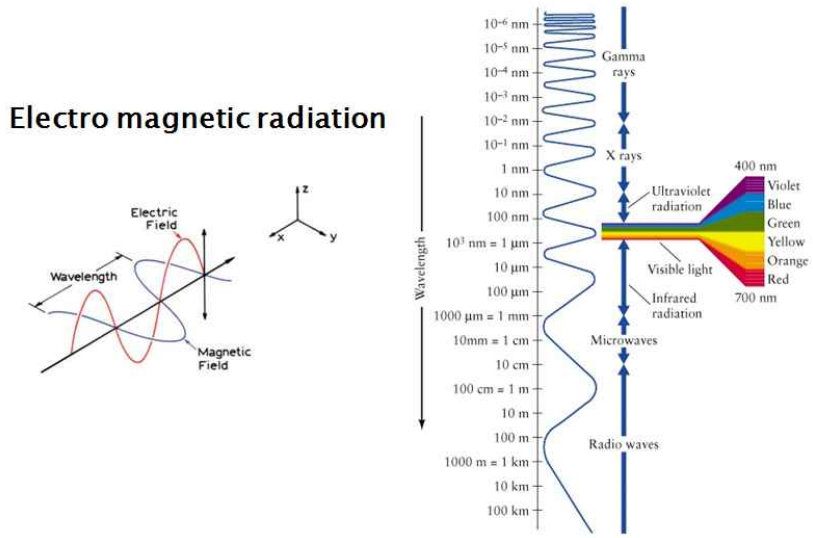


Fig. 23 Electromagnetic radiation and wavelength of each radiation.

Electromagnetic radiation is a combination of alternating electric and magnetic fields that pass through the space with a wave motion. Because radiation acts as a wave, it can be classified in terms of either wavelength of frequency, which are related by the following formula:

$$\nu = \frac{c}{\lambda} \quad \text{----------(14)}$$

where,

$\nu$ : frequency

$\lambda$ : wavelength

c : speed of light

It follows from the above formula that radiation with shorter wavelength has higher energy. In UV-Visible spectroscopy, the low-wavelength UV light has the highest energy. In some cases, this energy is sufficient to cause unexpected photochemical reactions when measuring samples (Skoog et al., 2007)

The ideal light source would cover a constant and high intensity over all wavelength with low noise and long-term stability. But such a source does not exist and two sources are normally used in UV-Visible spectrophotometers.

First is a deuterium arc lamp. Fig. 24 shows the external view and internal construction of a deuterium lamp. The anode has a unique structure covered with ceramic to prevent abnormal discharge, and the cathode has a highly durable electrode. Since a deuterium lamp uses the positive column flash or arc discharge, the cathode is shifted sideways and an aperture is located immediately in front of the anode so that high intensity is obtained. the aperture plate placed between anode and cathode may be used as an auxiliary electrode for lamps designed for low voltage lighting. But as seen in Fig. 25, D2 lamp can be used in only UV range and needs to be cooled as it is easy to be burned out. Besides, nucleic acid samples can be degraded by the continuos lighting. So the additional shutter should be used to block out the light except the moment of measurement.

The second light source is a pulse xenon lamp. It is widely used in the field of bio-measurements because it is free from the heat and does not need to be warmed up and there is no degradation of the sample by flashing only when measuring the sample. But it is more noisy and unstable than $D_2$ lamp because of the several sharp peaks.

For the measurement of fluorescence of samples, continuous xenon lamp and pulse xenon lamp have been generally used.

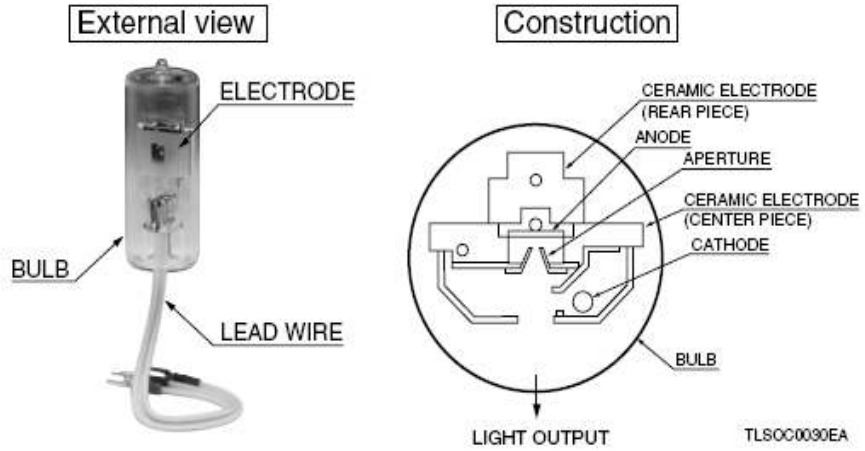


Fig. 24 External view and electrode construction of D2 lamp produced by Hamamatsu

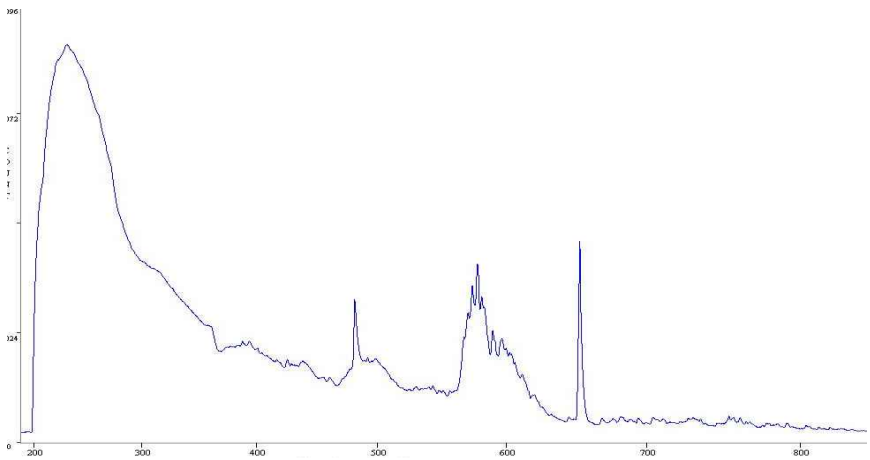


Fig. 25 Typical spectral distribution of D2 lamp

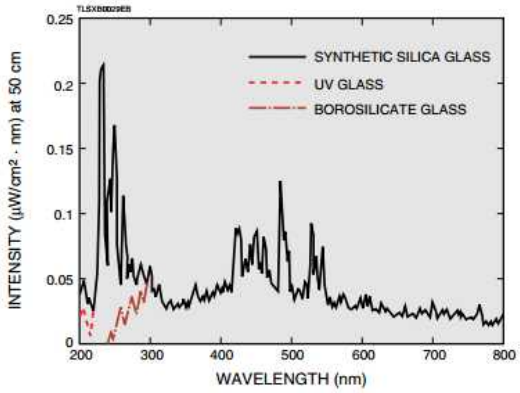


Fig. 26 Typical spectral distribution of flash xenon lamp (Hamamatsu)

These days, the light-emitting diode (LED) become more popular for dedicated instrument measuring fluorescence such as RT-PCR as it consumes very low power and it's life time is very long. When a LED is switched on, electrons are able to recombine with electron holes within the device, releasing energy in the form of photons. This effect is called electroluminescence and the color of the light is determined by the energy gap of the semiconductor.

LEDs present many advantages over incandescent light sources by lower energy consumption, longer lifetime, improved physical robustness, smaller size, faster switching and low cost.

For measuring fluorescence by excitation of sample, wavelength of light source must be selected using optical filter or mono-chromator. But if well optimized LED could be used, there is no need of wavelength selector as LED light can emit the light of specific wavelength and it can be used as the selected wavelength light source to measure fluorescence of DNA conjugated with fluorescence dye.

### 2.4.4 Detectors

There are various light detection devices. Ideally, detectors should give a linear response over a wide range with low noise and high sensitivity.

PMT is the mainly used for UV-Vis spectrometer and fluorescence spectrometer. Photo diode detectors become more popular with low-cost and high robustness. But these single channel sensor does not have ability to distinguish the wavelength of light and need the wavelength selector. In the field of monitoring or biological application, the fast measurement is very important as sample varies too fast and easily to be degraded. For this reason, polychromator which is able to separate the wavelength of transmitted light through the sample could be applied. In the polychromator, light detection should cover whole wavelength range in a fixed position and linear image sensor must be used for this application.

Normally two types of linear image sensors are used in spectroscopy. The first is photo diode array (PDA) and the second is charge coupled device (CCD). PDA is very stable, has low noise and covers wide dynamic range but it is relatively expensive. CCD is low cost, very sensitive but is more noisy than PDA. For measuring small amount nucleic acid, the signal intensity is very low and needs high sensitivity and noise could be removed by signal processing such as Savitzky-Golay smoothing. (Skoog et al., 2007)

Fig. 27 shows how to readout photoelectrons of CCD array. Before storing charge from each sense elements in a CCD to determine photon flux on that pixel, the charge must be transferred first to a readout node while maintaining the integrity of the charge packet. A fast and efficient charge-transfer process, as well as a rapid readout mechanism, are crucial to the function of CCDs as imaging

devices. When a large number of MOS capacitors are placed close together to form a sensor array, charge is moved across the device by manipulating voltages on the capacitor gates in a pattern that causes charge to spill from one capacitor to the next, or from one row of capacitors to the next. The translation of charge within the silicon is effectively coupled to clocked voltage patterns applied to the overlying electrode structure, the basis of the term "charge-coupled" device.

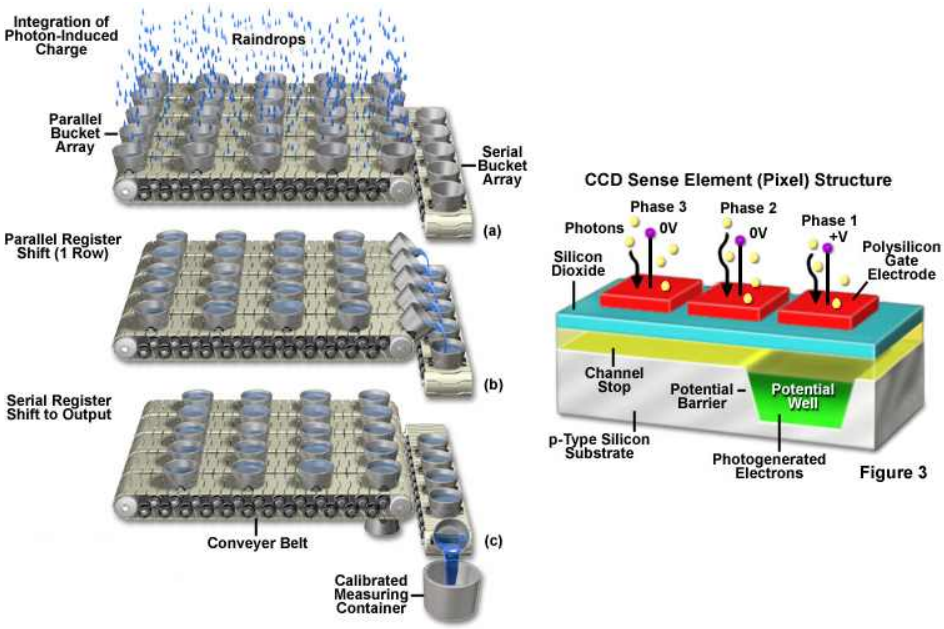


Fig. 27 Readout process of CCD detector (Olympus)

# III. Design of Optics

In this chapter, the process of design, optimization and verification of optics is presented to achieve the objectives of this study.

Optics design was basically performed using total internal reflection theories. And this design was optimized by checking the ray traced using optical simulation software. Finally, this design was verified by measuring various samples.

## 1. Introduction

To get the higher sensitivity, according to the Beer's law, the path length should be enlarged. If the beam could pass through the sample several times, path length inside of sample could be enlarged as shown in Fig. 28. To establish this concept, there must be a reflective component such as metallic mirror or window. Metallic mirror is an easy solution for doubling the path length but it can be easily damaged by repetitive cleaning which is not suitable for repetitive use.

If transparent reflector such as a window or thin film would be used, incident beam angle should not be normal to the reflector because about 98% beam may be transmitted through the reflector when entering at normal angle.

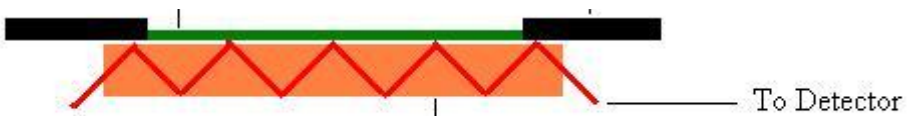


Fig. 28 Enlarging the path length inside of sample by multiple reflection

Thus, if the incident beam angle is over critical angle to the sample, beam will

be refracted and reflected because of different refractive index following the Snell's law. Therefore beam pass length can be longer over two times comparing normal incident beam and fluorescence light area from sample can be much wider by enlarging the beam path length.

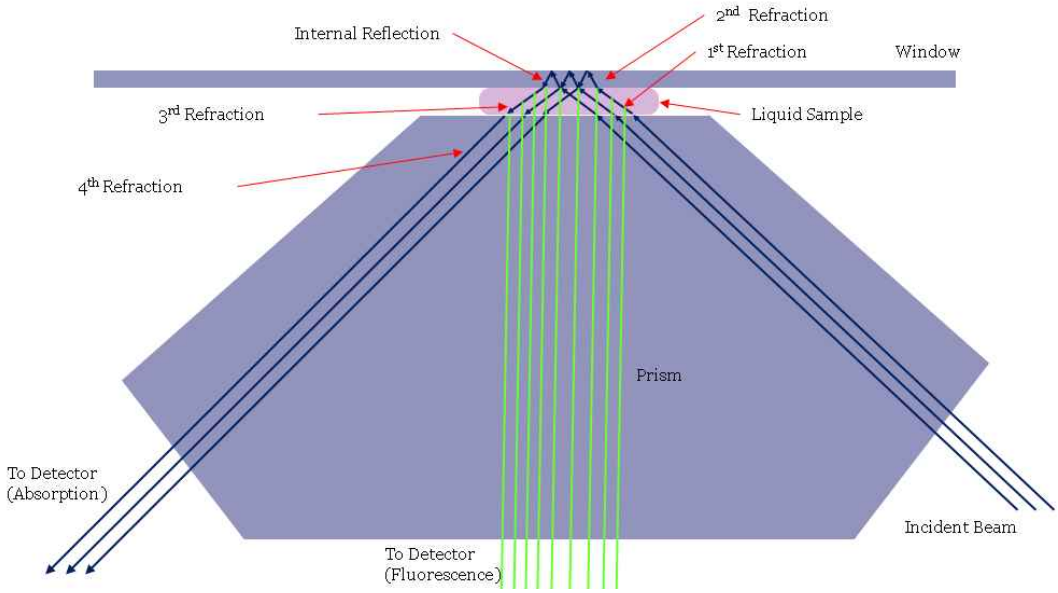


Fig. 29 The concept of optical geometry to enlarge the beam path length and to measure absorbance and fluorescence for micro-volume samples simultaneously

If the normal distance between the window and the prism is 1mm and sample is placed as rectangular shape with 1.5mm width and 0.67mm length and incident angle is 45°, beam path length could be about 2.83mm. The beam path length in this optics design is defined as formula 16.

$$n_1 \sin\theta = n_2 \sin\theta' \quad \text{----------(15)}$$

$$l = \frac{h}{\cos\theta'} = \frac{h}{\sqrt{1-\sin^2\theta'}} = \frac{h}{\sqrt{1-\left(\frac{n_1}{n_2}\right)^2 \sin^2\theta}} \quad \text{----------(16)}$$

where,

$h$ : sample height

$\theta$ : entrance angle

$\theta'$ : refracted angle

$n_1$ : refractive index of fused silica used for window and prism

$n_2$ : refractive index of sample

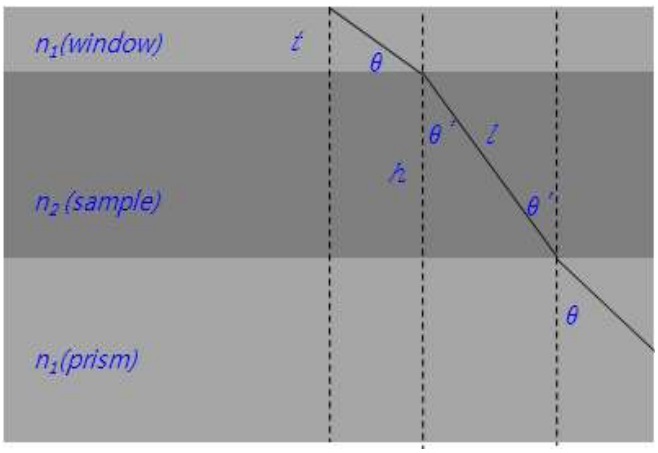


Fig. 30 Refracted light via sample between a window and a prism

If $h$ = 1 mm, and $n_1$= 1.5 and $n_2$ = 1.3, path length can be plotted as Fig.31.

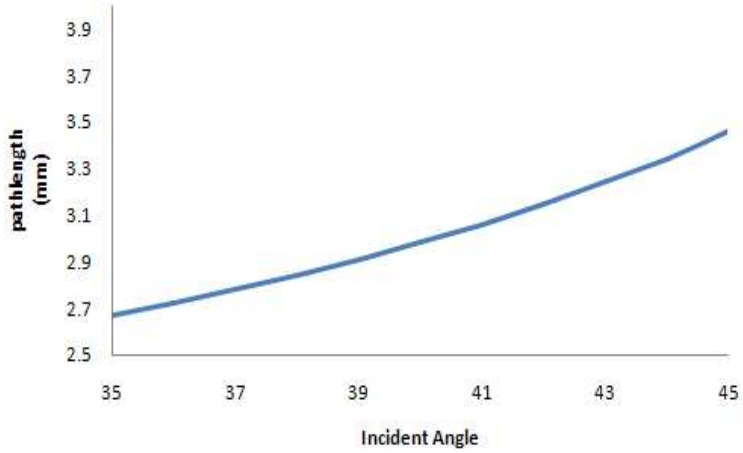


Fig. 31 Relation between path length and incident angle

# 2. Optics Design

## 2.1 Total Internal Reflection

Incident angle could be determined by prediction of the performance by total internal reflection at the border between window and air by Snell's law. To use the Snell's law, refractive index must be defined as refractive index depends on the wavelength. To measure spectrum data of nucleic acid, the material of optics needs to be transparent for UV beam. Fused silica has been widely used as a material for lens or window in UV region. Fused silica is a non-crystalline form of silicon dioxide. It’s highly cross linked three dimensional structure enables it to endure high temperature and to give low thermal expansion coefficient.

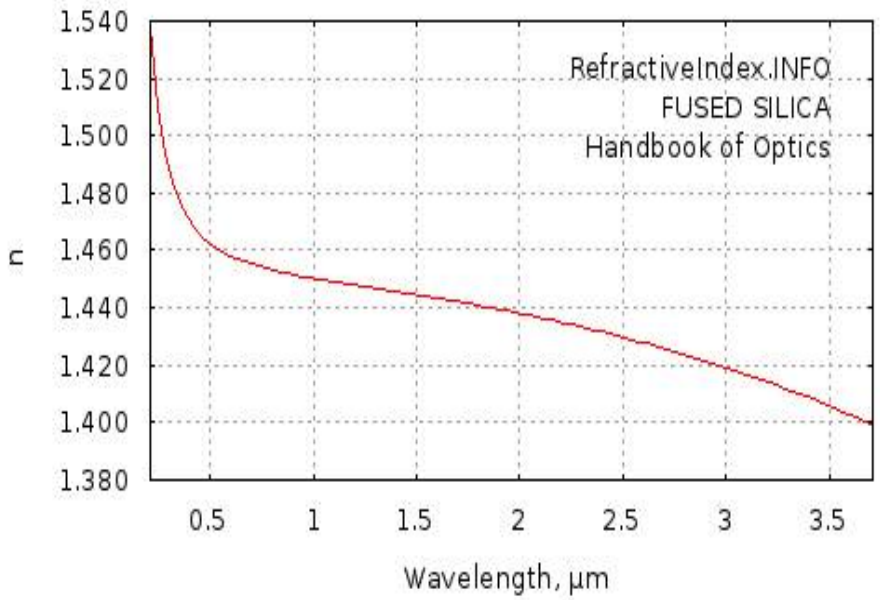


Fig. 32 Refractive index curve of fused silica on each wavelength (Handbook of Optics)

Refractive index is the function of wavelength as shown in Fig. 32. Thus, to find the optimal geometry of optics by Snell's law, refractive index must be fixed. In this study, all optics design should be optimized to UV region for measuring nucleic acid and bio materials. In this area, refractive index varies from 1.488 to 1.5. The calculation result shows that incident angle must be over 42.5$^{o}$ because refraction angle in air could not be calculated using the Snell's law when incident angle is over 42.5$^{o}$ as listed in Table 3.

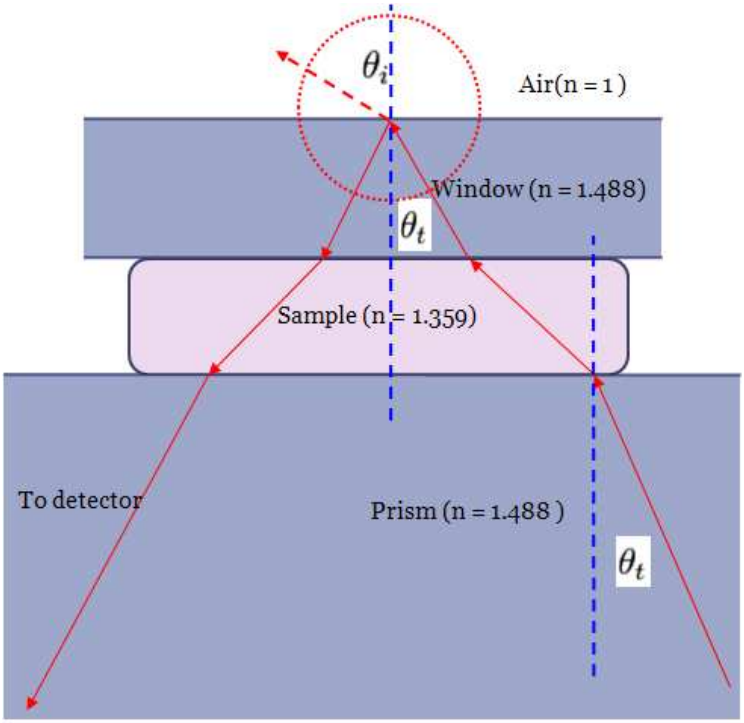


Fig. 33 Total internal reflection at the surface of window by the difference of refractive index between the air and fused silica window

Table 3. Optimum incident angle determined by total internal reflection

| Thi | Sin(Thi) | n1 | n2 | Sin(i) | I (Air) |
|---|---|---|---|---|---|
| 30 | 0.5 | 1.488 | 1 | 0.744 | 48.07328 |
| 30.5 | 0.507538 | 1.488 | 1 | 0.755217 | 49.04434 |
| 31 | 0.515038 | 1.488 | 1 | 0.766377 | 50.02962 |
| 31.5 | 0.522499 | 1.488 | 1 | 0.777478 | 51.03023 |
| 32 | 0.529919 | 1.488 | 1 | 0.78852 | 52.0474 |
| 32.5 | 0.5373 | 1.488 | 1 | 0.799502 | 53.08256 |
| 33 | 0.544639 | 1.488 | 1 | 0.810423 | 54.13727 |
| 33.5 | 0.551937 | 1.488 | 1 | 0.821282 | 55.21336 |
| 34 | 0.559193 | 1.488 | 1 | 0.832079 | 56.3129 |
| 34.5 | 0.566406 | 1.488 | 1 | 0.842812 | 57.43831 |
| 35 | 0.573576 | 1.488 | 1 | 0.853482 | 58.59241 |
| 35.5 | 0.580703 | 1.488 | 1 | 0.864086 | 59.7785 |
| 36 | 0.587785 | 1.488 | 1 | 0.874624 | 61.00056 |
| 36.5 | 0.594823 | 1.488 | 1 | 0.885096 | 62.26338 |
| 37 | 0.601815 | 1.488 | 1 | 0.895501 | 63.57282 |
| 37.5 | 0.608761 | 1.488 | 1 | 0.905837 | 64.93625 |
| 38 | 0.615661 | 1.488 | 1 | 0.916104 | 66.36304 |
| 38.5 | 0.622515 | 1.488 | 1 | 0.926302 | 67.86548 |
| 39 | 0.62932 | 1.488 | 1 | 0.936429 | 69.46021 |
| 39.5 | 0.636078 | 1.488 | 1 | 0.946484 | 71.17071 |
| 40 | 0.642788 | 1.488 | 1 | 0.956468 | 73.03201 |
| 40.5 | 0.649448 | 1.488 | 1 | 0.966379 | 75.10058 |
| 41 | 0.656059 | 1.488 | 1 | 0.976216 | 77.47879 |
| 41.5 | 0.66262 | 1.488 | 1 | 0.985979 | 80.39402 |
| 42 | 0.669131 | 1.488 | 1 | 0.995666 | 84.66393 |
| **42.5** | **0.67559** | **1.488** | **1** | **1.005278** | **#NUM!** |
| **43** | **0.681998** | **1.488** | **1** | **1.014814** | **#NUM!** |
| **43.5** | **0.688355** | **1.488** | **1** | **1.024272** | **#NUM!** |
| **44** | **0.694658** | **1.488** | **1** | **1.033652** | **#NUM!** |

## 2.2 Polarized Reflection on Surfaces

According to the Fresnel's law of reflection, light on the surface can be reflected with p and s polarity even the light passes through the media by snell's law. And the reflectance of each component is related to the incident angle. If incident angle is bigger than the critical angle, the beam internally reflects from the surface between the prism and sample, it may act like a stray light in optics and affect the accuracy of the measurement.

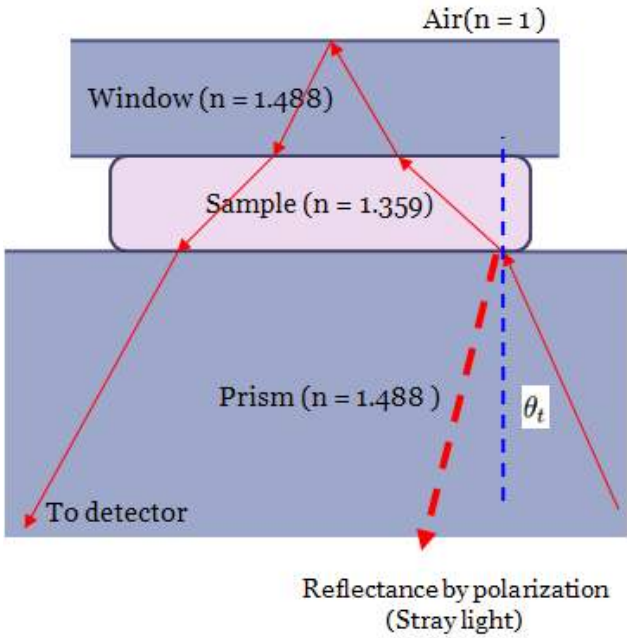


Fig. 34 Internal reflection at the surface between the sample and fused silica prism

Using the Fresnel's law, internal reflectance can be predicted and plotted as Fig. 35. According to the results of this chart, incident angle must be minimized in

order to minimize internal reflection between the prism and sample. But considering the result from total internal reflection on the layer between window and air, incident angle must be over 42.5. Considering the machining of optics, incident angle is determined as 45$^{o}$ and thickness of window is 0.2mm. The path length of this design was calculated as 2.83mm when the sample height is 1 mm.

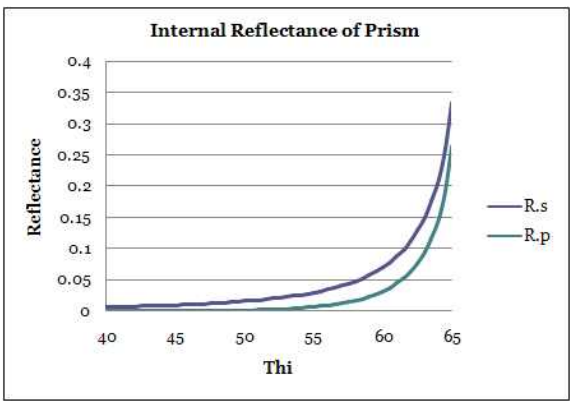


Fig. 35 Reflectance curve of P and S polarized beam with different entrance angle (thi) to the prism

## 2.3 Analysis of Optics by Optical Simulation

To analyze of the optics with various dimensions of sample and optical components, ray tracing method was applied by using TracePro 6.0 from Lambda Research (USA). In this simulation, transmitted beam, fluorescence beam and stray light could be traced in different conditions. Especially, minimum sample volume could be determined by checking the unexpected stray light on the optics and by optimizing the physical dimensions when sample height varied from 0.1 to

1.0 mm.

To simulate the optics using this software, several parameters and properties should be determined in previous. For the materials of window, prism and lenses fused silica was selected and it's refractive index and absorption coefficient were as shown on Fig. 36. The lenses used on this simulation was plano-convex type and several parameters are shown on Fig. 37. The light source was determined as point source with diameter of 0.6mm for the light output because the optical fiber core is 600 $um$ dia. The detailed parameters of light source are shown on Fig. 38. The 'Water' was selected for the material of sample as shown in Fig. 39 because nucleic acids are normally diluted to TE buffer of which main component is distilled water.

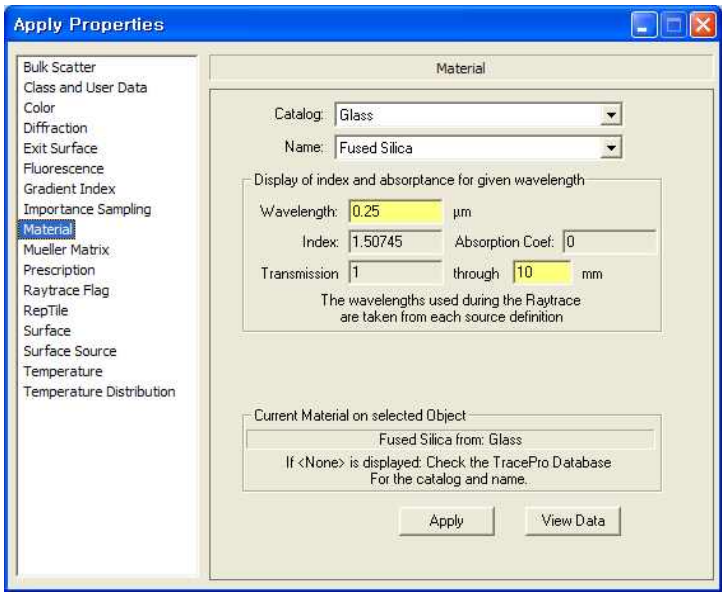


Fig. 36 Parameters of prism in optical simulation

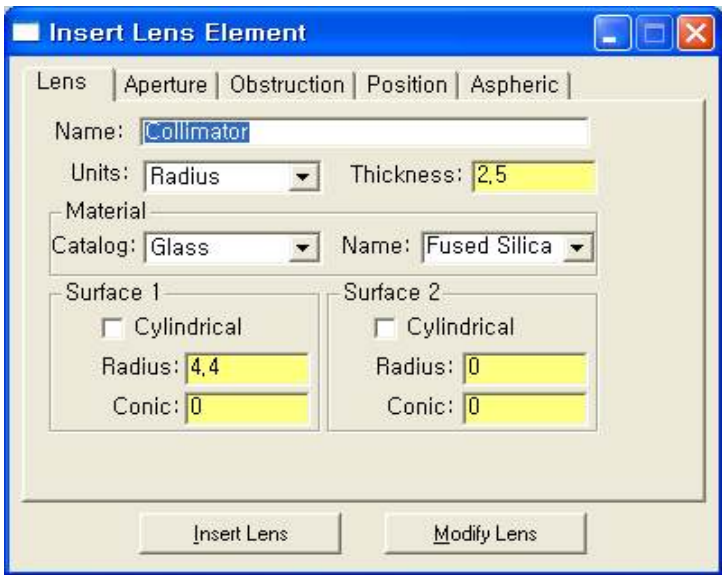


Fig. 37 Parameters of collimating lens in optical simulation

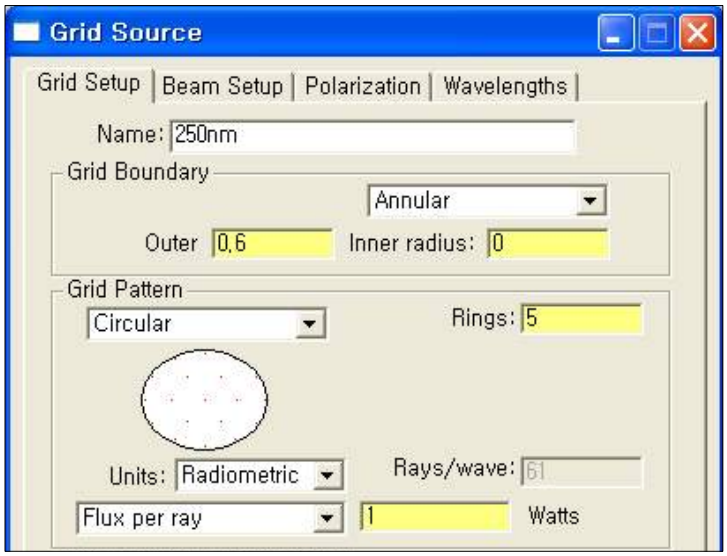


Fig. 38 Parameters of light source in optical simulation

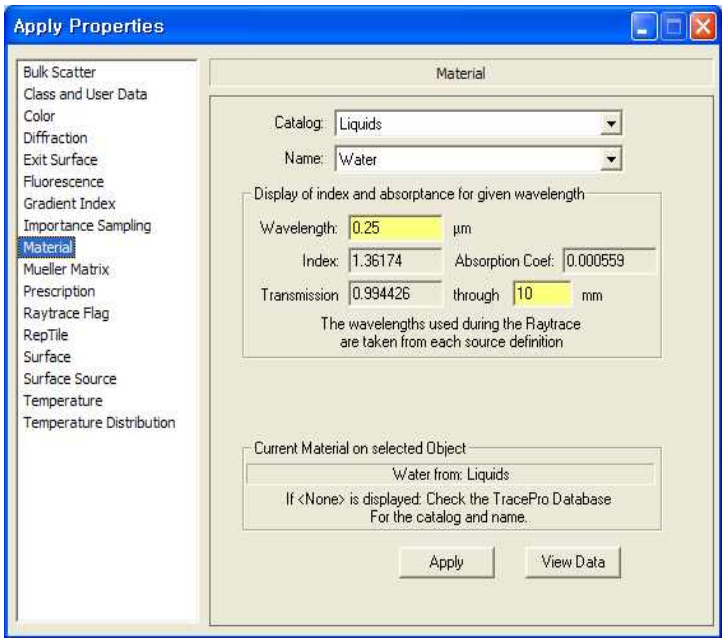


Fig. 39 Material properties of sample (water) in optical simulation

Various optical alignments on the software can be easily checked by seeing the direct positioning the optical components. As shown in Fig. 40, the sample shape should be rectangular to minimize the sample size.

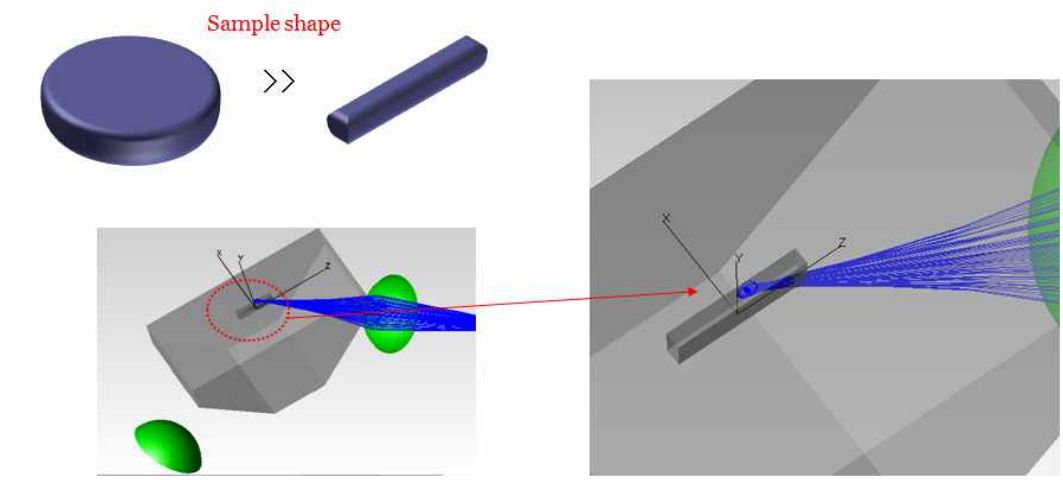


Fig. 40 The shape of sample to minimize the volume of sample

Fig. 41 and 42 show that the results of simulation when the sample height is 0.1 mm. In this result, if the beam height is 0.1 mm, the sample volume can reach to 0.09 $ul$ in simulation. The detailed trace of ray between the prism, sample and window can be checked on Fig. 42. In Fig. 42, small numbers of rays are transmitted through the window as the incident angle is under the level of total internal reflection. But these rays is not transferred to the detector and can be neglected for measuring absorbance of sample. In Fig. 43, Fig 44, If a sample's width is under 1.8mm, large numbers of stray light appeared as shown in Fig. 44 and it may not be possible to measure correct absorbance because of low light intensity transferred to the detector.

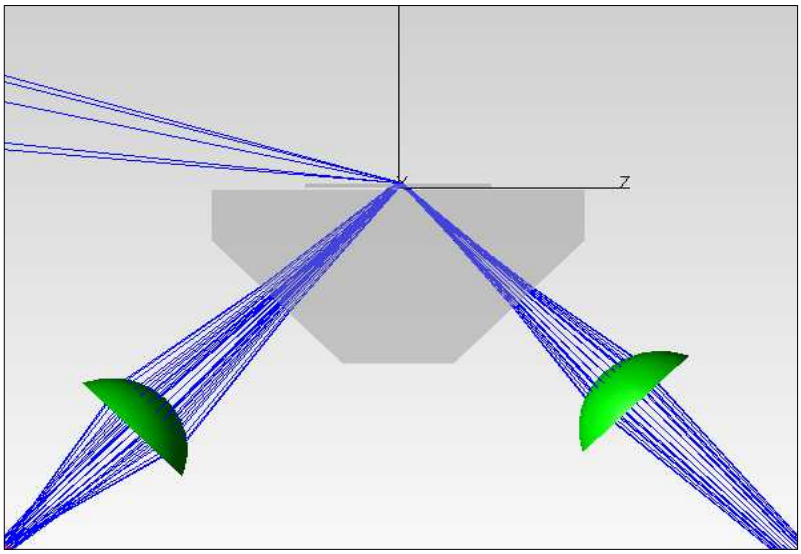


Fig. 41 Ray tracing in condition of 0.1mm sample height

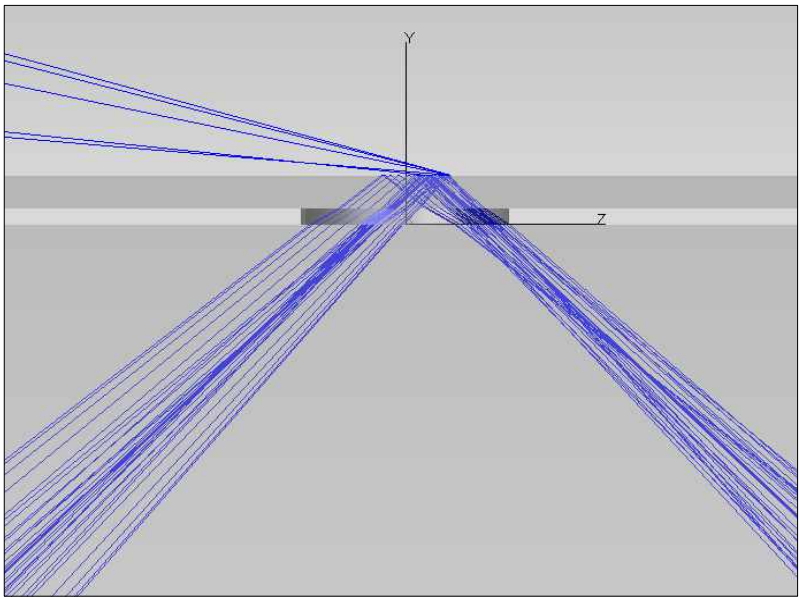


Fig. 42 Ray tracing in condition of 0.1mm sample height

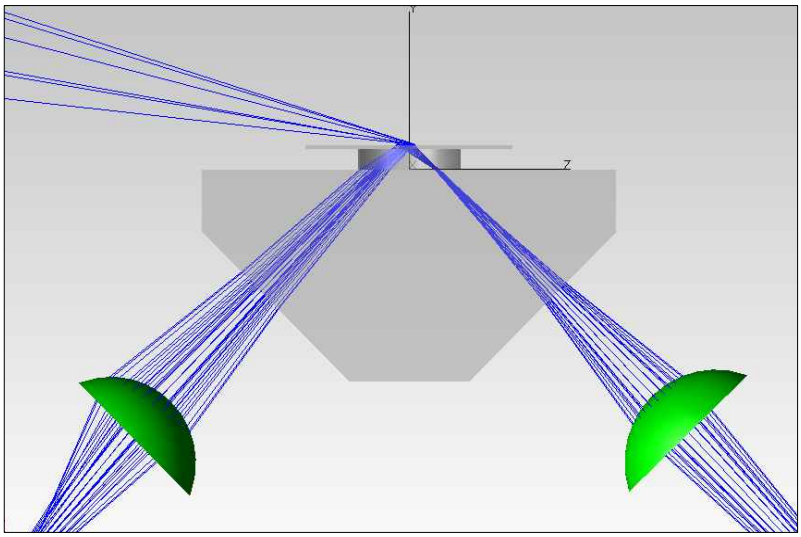


Fig. 43 Ray tracing in condition of 1 mm sample height

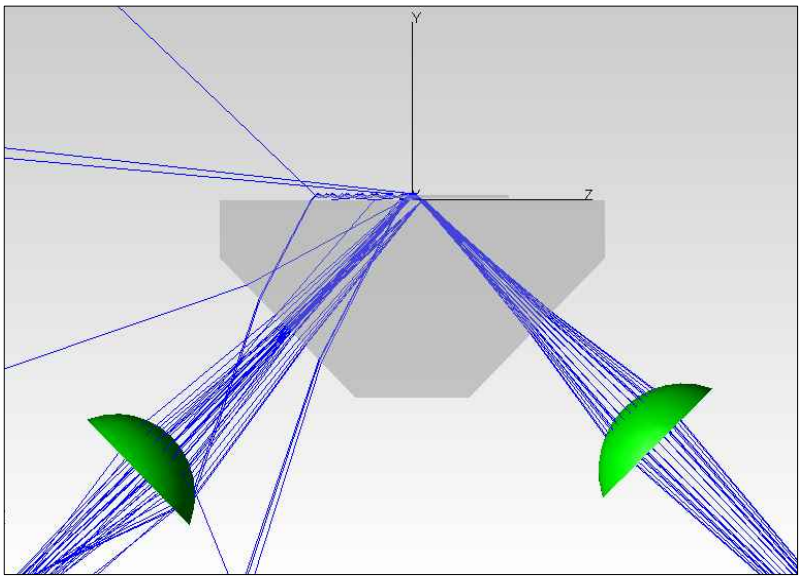


Fig. 44 Scattering resulted from incorrect sample size

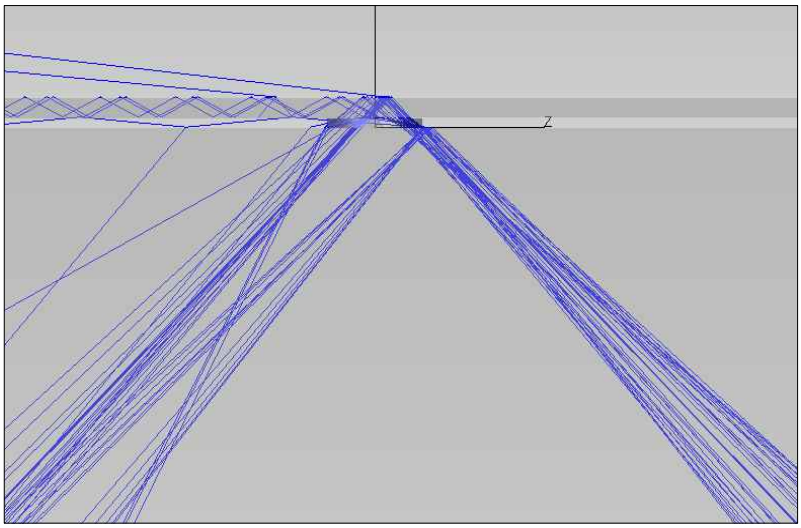

Fig. 45 Scattering resulted from incorrect sample size

The results of predicted minimum sample volume at each sample conditions are listed on Table 4. It shows that the usable sample volume can be minimized to $0.09ul$ by using this optics design.

Table 4. Sample volume determined at each sample height

| Height (mm) | Path length (mm) | Depth (mm) | Width (mm) | Volume (ul) |
|---|---|---|---|---|
| 0.1 | 0.283 | 0.5 | 1.8 | 0.09 |
| 0.2 | 0.566 | 0.5 | 2.2 | 0.22 |
| 0.4 | 1.131 | 0.5 | 2.5 | 0.5 |
| 0.6 | 1.697 | 0.5 | 3.5 | 1.05 |
| 0.8 | 2.263 | 0.5 | 4 | 1.6 |
| 1 | 2.828 | 0.5 | 4 | 2.83 |

To predict the effect of fluorescence light from sample to the absorption detector, ray tracing of fluorescence was peformed as Fig. 46. In this simulation, the fluorescence light spreaded to all direction and there is very low possibility of entrance to the detector for absorption measurement.

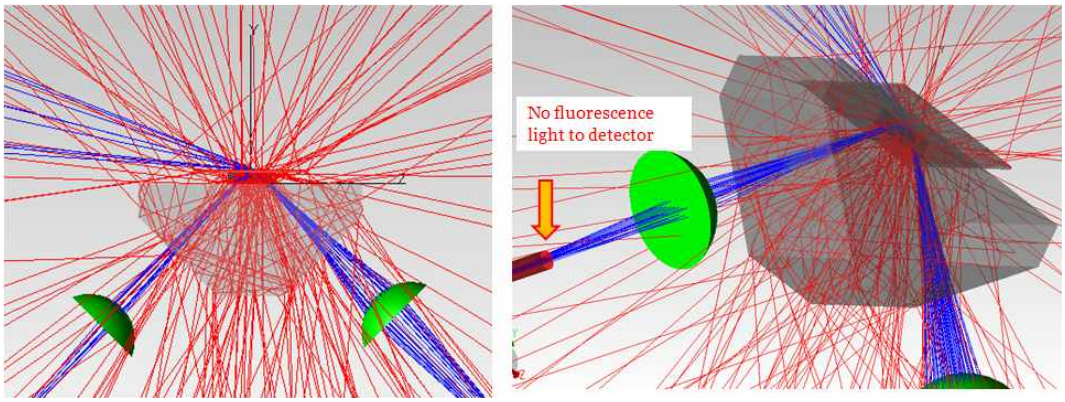


Fig. 46 Fluorescence light spreaded from sample in ray tracing

# 3. Verification of Optics Design by Measurement of Sample

## 3.1 Materials and Method

To verify the optics design, prism was machined in Hong-Sung Optics, Korean optical component manufacturer. Fused silica in commercial quality was used and machined prism is shown in Fig. 47. A quartz cover slip from SPI was used as a reflecting window. The 6 watts light source in which D2 and halogen lamp are assembled called 'FiberLight' from Heraeus was used for light source. SM 440 spectrograph from Korea Spectral Products (KSP) was used for measuring the spectrum of sample. SM 440 is a CCD type spectrograph has 1.5nm resolution with 190~1100nm wavelength range. To transfer the light, optical fiber whose core size is 600um was connected with SM905 connector. To adjust the normal distance from prism to the window, 3-axis translation stage was employed for optical alignment. The fabricated experimental device is shown in Fig. 48.

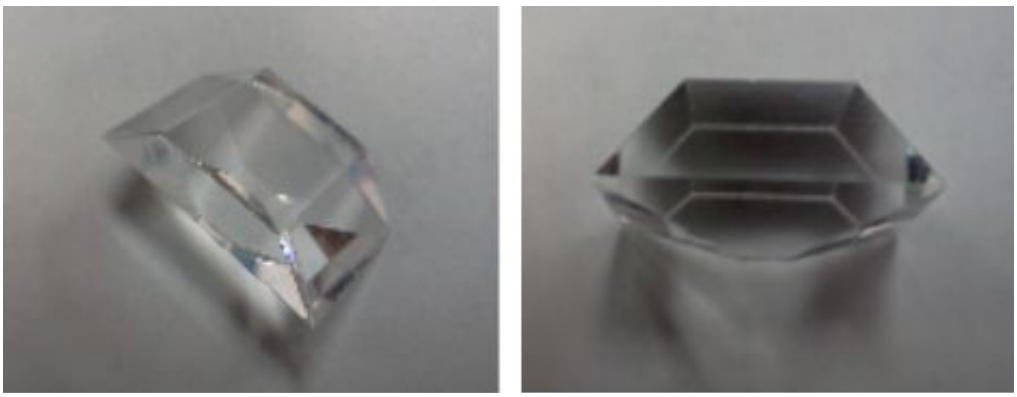

Fig. 47 Machined prism based on the optics design

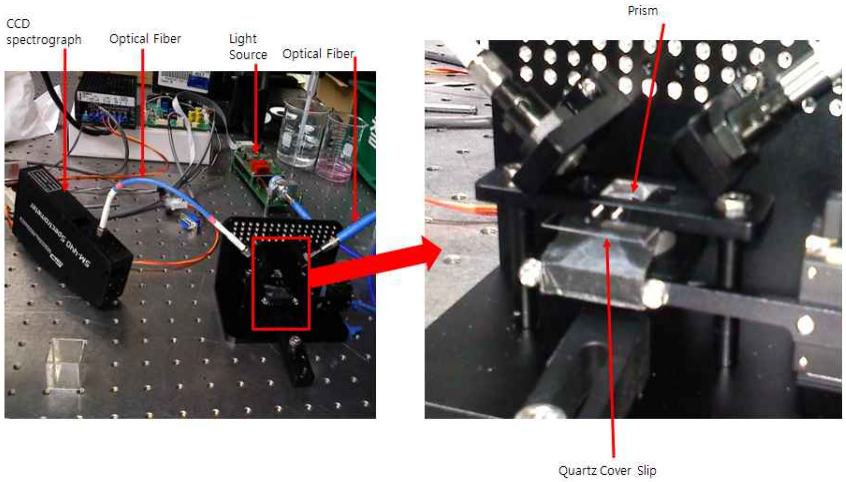


Fig. 48 Fabricated experimental equipment for verification of optics design

Verification was performed by comparing the results of the several UV-Vis spectrometers. Cary 300 UV-Vis spectrometer from Agilent, S-3100 UV-Vis spectrophotometer from SCINCO, Nano-Drop from Thermo Scientific were used to acquire the spectra of same samples.

At first, a high concentrated colored sample was used for the verification of optics design by checking the similarity between the predicted path length design and the real path length measured from fabricated experimental equipment.

And Calf Thymus DNA, Calf Liver RNA were obtained from Sigma. TE buffer (10mM Tris HCl, 1mM EDTA pH 8.0) was used for dissolution of the sample. These nucleic acid samples were used for verification of reliability of this optics design.

Finally 20 $ng/\mu\ell$ of Calf Thyums DNA from 0.1 $\mu\ell$ to 1 $\mu\ell$ were measured to verify optical simulation and to determine minimum sample.

## 3.2 Results and Discussion

### 3.2.1 Verification of optics design in terms of the path length

The absorption spectrum of orange colored sample measured by Cary 300 spectrometer and the maximum peak is 3.2 as shown in Fig. 49. Fig. 50 shows the spectrum measured by the prorototype spectrometer with the designed optical components in this study. As shown in this spectrum, maximum absorbance is 0.9. The path length of the system fabricated can be determined by figuring out the ratio of maximum absorbances between two instruments. Simply, it could be determined by 10 × 0.9/3.2 = 2.81 mm considering the beam path length of Cary 300 is 10 mm. In previous optics design, the path length was predicted to 2.83mm. Thus the error between the prediction and measurement was 0.02mm which is under 1%.

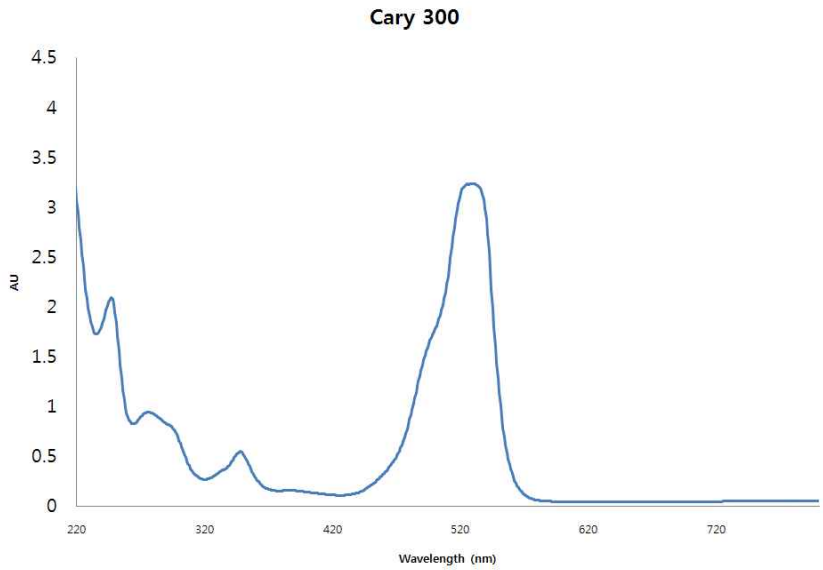


Fig. 49 Absorption spectrum measured by Cary 300 spectrometer

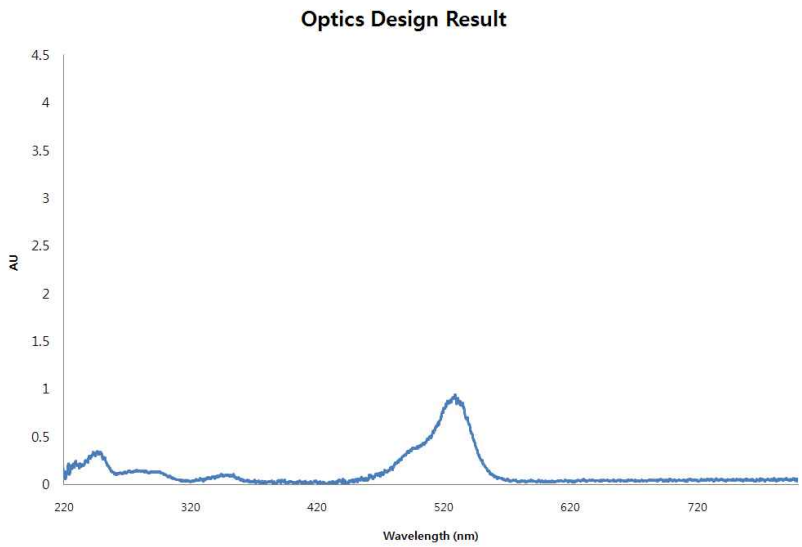


Fig. 50 Absorption spectrum measured by the prototype spectrophotometer

### 3.2.2 Verification of optics design in terms of the accuracy

Fig. 51 and 52 and Table 5, 6 show that the comparison results between the conventional devices and fabricated test equipment. From these results, standard deviation of purity for 4 devices is 0.04 in DNA and 0.02 in RNA.

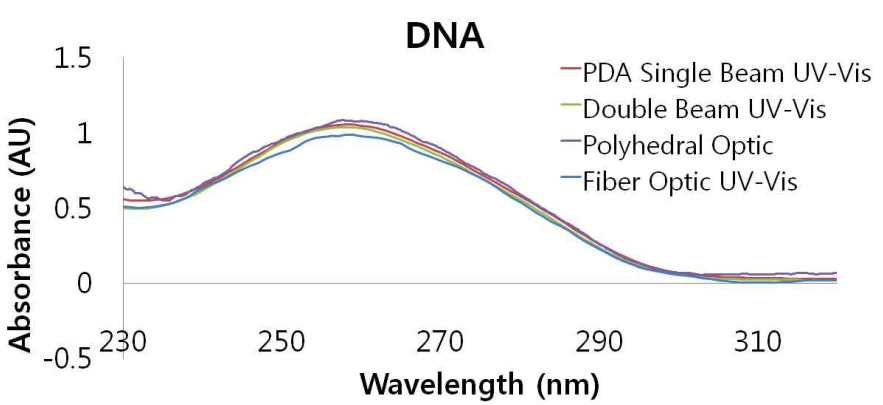


Fig. 51 DNA spectra measured by four spectrometers

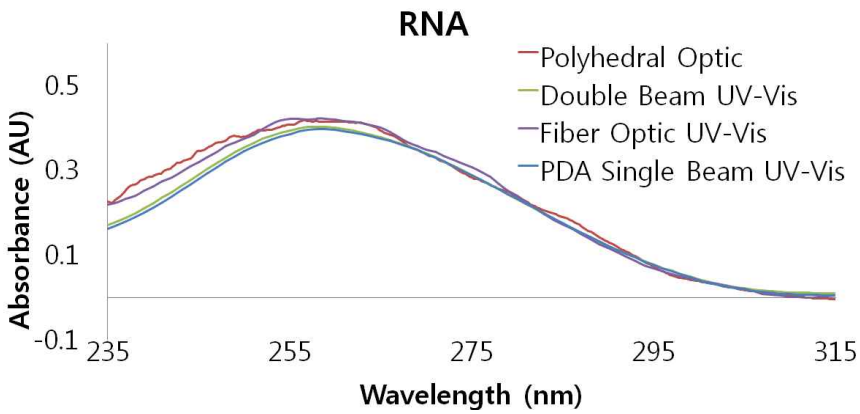


Fig. 52 RNA spectra measured by four spectrometers

Table 5. Purity measurement results of DNA using several instruments.

| DNA | Double Beam | PDA Single beam | Fiber Optic System | Developed Optic | STDEV |
|---|---|---|---|---|---|
| Purity | 1.86 | 1.81 | 1.82 | 1.84 | 0.04 |
| A260 | 1.029 | 1.047 | 0.979 | 1.078 | 0.04 |
| A280 | 0.554 | 0.578 | 0.538 | 0.586 | 0.02 |

Table 6. Purity measurement results of RNA using several instruments.

| RNA | Double Beam | PDA Single beam | Fiber Optic System | Developed Optic | STDEV |
|---|---|---|---|---|---|
| Purity | 1.73 | 1.70 | 1.75 | 1.75 | 0.02 |
| A260 | 0.400 | 0.395 | 0.419 | 0.414 | 0.01 |
| A280 | 0.232 | 0.232 | 0.24 | 0.236 | 0.004 |

### 3.2.3 Verification of optics design in terms of the sample volume

Fig. 53 shows that the absorbance measurement results of various sample heights (0.1mm ~ 1.0 mm). In this experiment, 0.1 mm sample height corresponds to 0.283 mm path length and 1 mm to 2.828 mm.

Fig. 54, 55 show the linearity curves from 0.1mm to 1 mm and from 0.2 mm to 1mm of sample height. The sample volume is 0.1 $\mu\ell$ for 0.1 mm sample height and 0.2 $\mu\ell$ for 0.2 mm sample height. In these results, the linearity includes the result of 0.1mm sample height is 0.9952 in R value and it can be enhanced to 0.9998 by excluding the result of 0.1mm sample height.

Considering the linearity of experimental result, the minimum sample volume in real experiment was determined as $0.2\mu\ell$ .

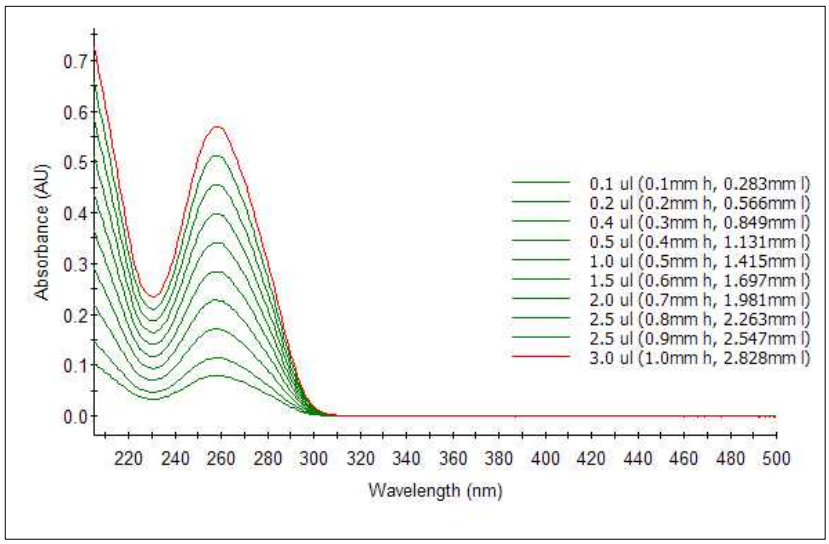


Fig. 53 Absorbance spectra with different height of samples measured by the prototype spectrometer

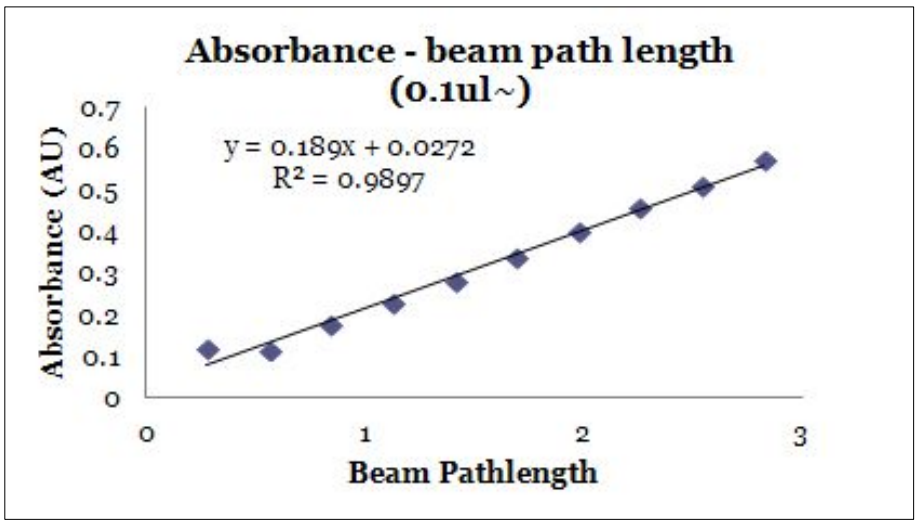


Fig. 54 Absorbance results along the change of beam path length (0.1ul ~)

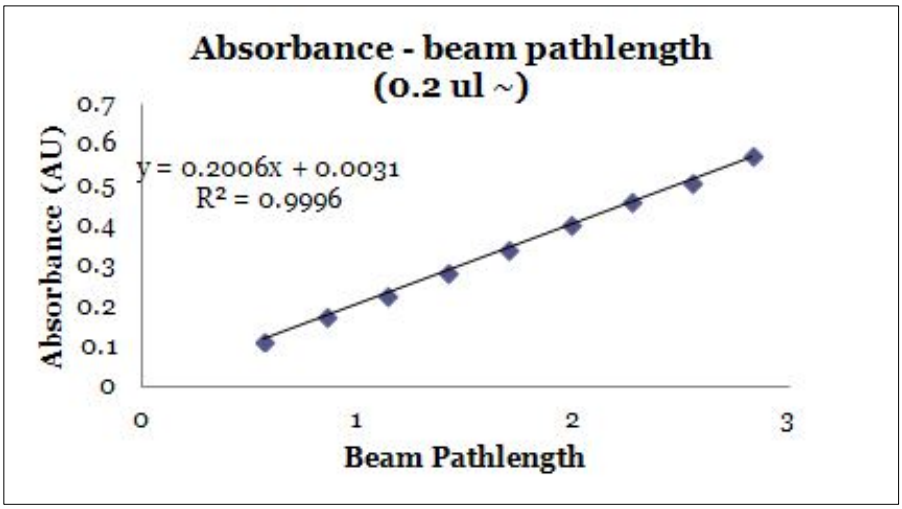


Fig. 55 Absorbance results along the change of beam path length (0.2ul ~)

## 4. Conclusion

In this section, optics design using total internal reflection was proposed to measure fluorescence and absorbance spectra of small amount sample with high sensitivity, stability and flexibility.

To design the optics, Snell's law of refraction and Fresnel's law of reflection was applied and incident angle of light was determined as 42.5$^{o}$. Considering machining of prism, incident angle was set to 45$^{o}$ and normal distance between the window and prism was fixed to 1mm. From the design of the optics, path length of this optics design was estimated to 2.83mm.

To optimize the sample size, optical simulation was peformed by ray tracing in various sample heights on the designed optical system and the minimum sample volume could be predicted to 0.09 $u\ell$

To verify optics design, experimental equipment was fabricated with a light source, aligning tools, several optical components and a spectrograph. A high concentration orange color sample was measured for comparing the path length of fabricated equipment with that of conventional UV-Vis spectrometer. The maximum absorbance value of conventional UV-Vis spectrometer was 3.2 and that of fabricated equipment by new optics design was 0.9. The ratio between two systems is 0.281 and the beam path length of new optics design could be determined to 2.81mm. The error between the measurement and prediction was 0.02mm. And Calf Tymus DNA and Calf River DNA samples were measured by fabricated test equipment and the measurement results were also compared with those of 3 different type of conventional UV-Vis spectrometers. The standard deviation between 4 devices was 0.04 for DNA and 0.02 for RNA. To check the

minimum sample volume on the designed optics, various DNA samples with different volume levels and different path length were measured. The test results showed that the sample volume could be minimized to 0.2 $u\ell$ in actual experiment. There was a difference of minimum sample volume between the simulation and real experiment. It is because of the humane error by sampling a small volume samples such as 0.1 $u\ell$ by hand and the low intensity caused by short path length and physical difference on optical alignment in real experiment.

# Ⅵ. Development of Synchronous Spectrometer

In this chapter, the development process of spectrometer is presented for simultaneous measurement of absorbance and fluorescence spectrum. This spectrometer was integrated based on the optimized optical components and several electronics and mechanics. To evaluate the system, various samples were measured and several statistical data were compared with existing system to show that the developed system has enhanced performances.

## 1. Introduction

Fig. 56 is the conceptual diagram of this system. The light source for absorption measurement is a pulse xenon lamp not to degrade bio sample by flashing only when measuring the samples. And LEDs are used for measuring the fluorescence. Optical filters also can be used but they need to be selected whenever changing the sample by driving filter wheel. In this study, for the robustness of system, UV, Blue and White LEDs are selected not to move the filter wheel. These lamps are controlled by PC software.

Light from the light source is transferred by optical fibers and passes through the prism and sample. And it is reflected from the last surface of quartz window.

There are two slits for measurement of fluorescence and absorption. Normally, fluorescence spectrum bandwidth is about 10nm and there is no need of narrow input slit of spectrograph. But for the absorption measurement, input slit should be narrow as typical spectral peaks are sharp and they should be distinguished for exact qualification. Thus, there must be two different size input slits.

For the dispersion of the light, holographic grating was used for each spectra

and dual CCDs are mounted for measuring dispersed lights.

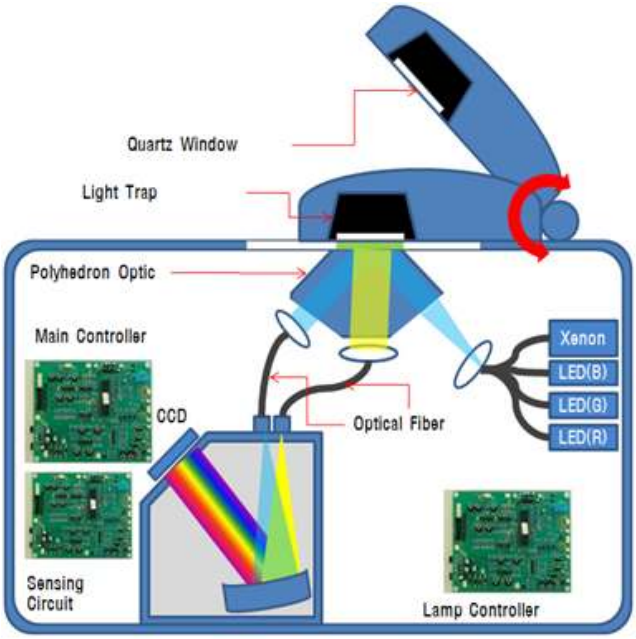


Fig. 56 System diagram for synchronous measurement of absorbance and fluorescence spectrum

Fig. 57 shows the block diagram of system control. All electronics are controlled by PC software connected with main controller by TCP-IP communication. After measuring the light intensity from the device, quantification of nucleic acid can be peformed by PC software.

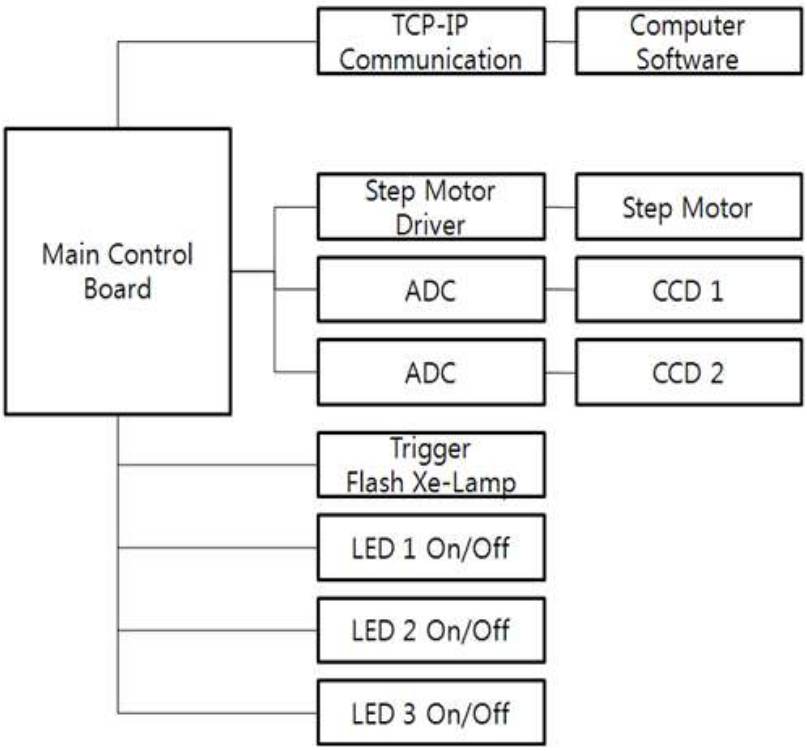


Fig. 57 Block diagram of system controls by main control board.

## 2. Development of Prototype

### 2.1 Light Sources

PAX-602-4P model of flash xenon lamp by Perkin-Elmer was used for absorption measurement. The life time of this lamp is over $2.0\times 10^9$ flashes and average output power is 6 watts. It covers wavelength range from 120nm to 2,000nm. To turn on the lamp, 5V triggering electronic circuit controller was fabricated. As mentioned before, the pulse lamp's flash time is about 1ms and does not cause the photo bleaching or degradation of bio samples.

UV, white and blue LEDs by Seoul Optodevice were used for measurement of fluorescence spectrum. The advantages of LED are no need of warming up time and additional cooling device. And the LEDs generate the beam of specific wavelength and can be used as a excitation light source without dispersing unit such as an optical filter or a grating. But if the energy gap between the excitation and the emission is very narrow under 20nm, band pass filter must be attached not to let the emission spectrum over-layed by the excited wavelength range. White LED was applied for total visible fluorescence measurement and UV LED was to excite the sample conjugated with the fluorescence dyes reacted with ultraviolet light such as Fluorescamine dye. Blue LED has been widely used as almost fluorescence dye can be excited by 400 ~ 500 nm light. Fig. 65, 66, 67 show the spectral distribution of each LED.

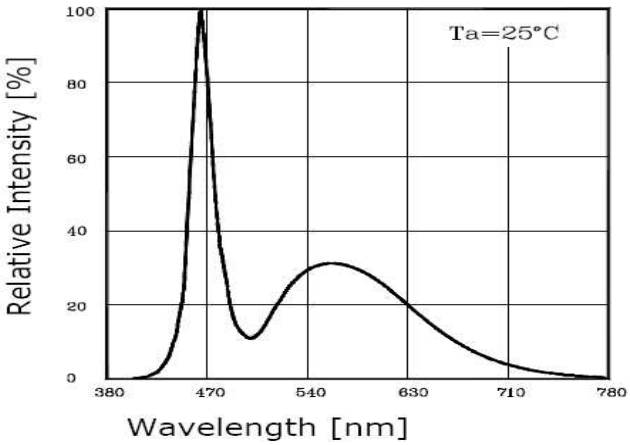


Fig. 58 Spectral distribution of white LED of the prototype spectrophotometer.

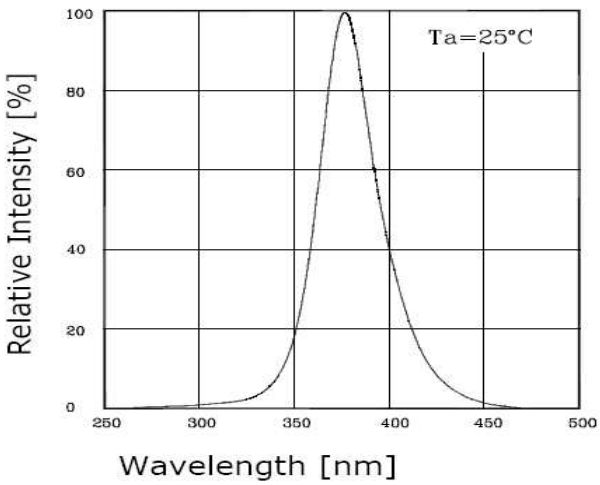


Fig. 59 Spectral distribution of UV LED of the prototype spectrophotometer

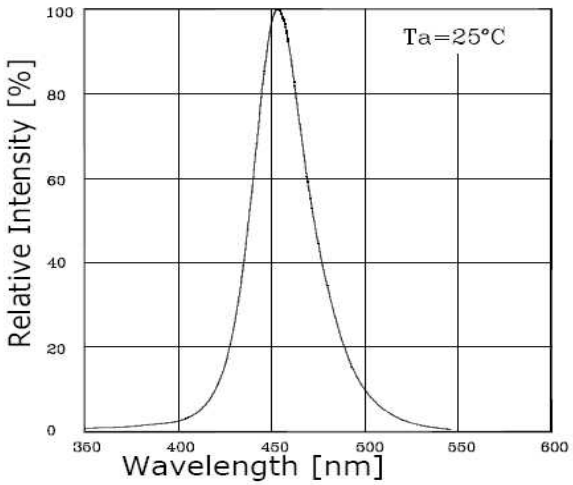


Fig. 60 Spectral distribution of blue LED of the prototype spectrophotometer

## 2.2 Optical Fibers

To transfer and focus the light from each light sources in a confined space, the optical fiber should be used as there is no need of optical components such as mirror or beam splitters.

In this study, total four light sources should be focussed to the sample between the prism and window and the optical fibers was fabricated as multi-plex type as shown in Fig. 61. The material of each core was fused silica and core size was 600um dia. And several factors of optical fiber are listed in Table 7.

Fig. 61 Multi-plex type optical fiber module for several light sources

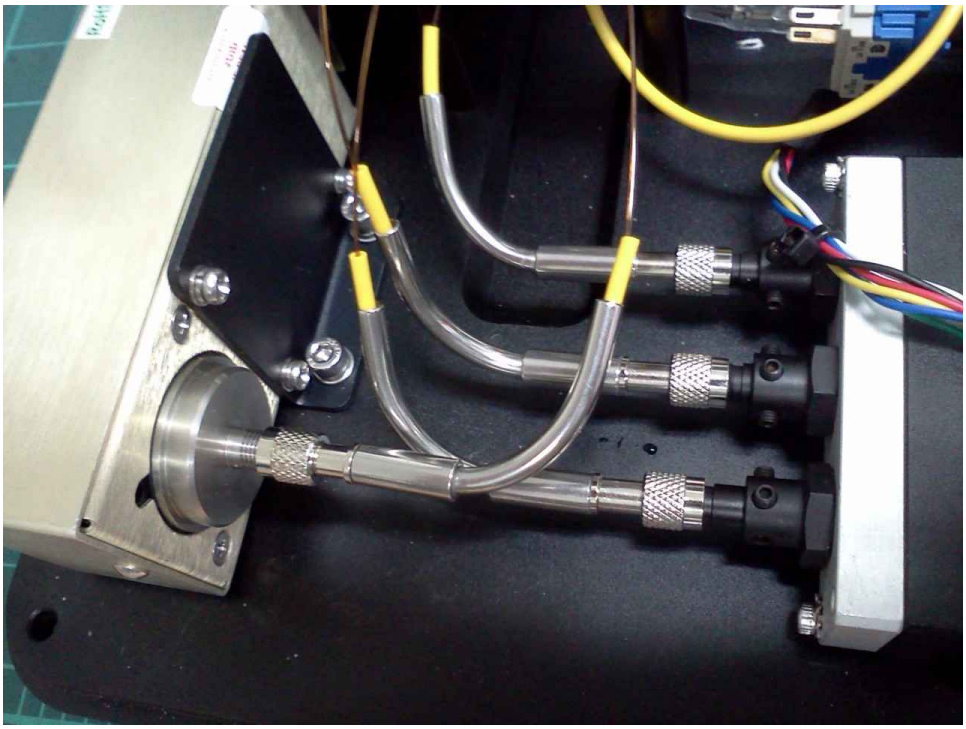

Fig. 62 Optical fiber connected with light sources

Table 7. The specifications of optical fiber used in this study

| Items | Values |
|---|---|
| Material | Fused Silica |
| Jacket | Not Applied |
| Connector Type | SMA 905 |
| Core Size | 600um |
| N.A | 0.22 |
| Acceptance Angle | 25.4 |

## 2.3 Spectrograph

The grating used in this development was 523-03-120 from Horiba Jobin-Yvon. This crating is a concave holographic grating and main factors for designing spectrograph are shown in Fig. 63 and Table 8. Fig. 64 shows how to acquire dual images using one grating. The on-axis dispersed light is for measuring absorbance and off-axis dispersed light is for measuring fluorescence. Fig. 65 shows the fabricated spectrograph on this research. But its size is too big for integration of system and could not be used. So small size SM 200 spectrographs from Korea Spectral Products were modified to measure individually fluorescence and absorption spectrum.

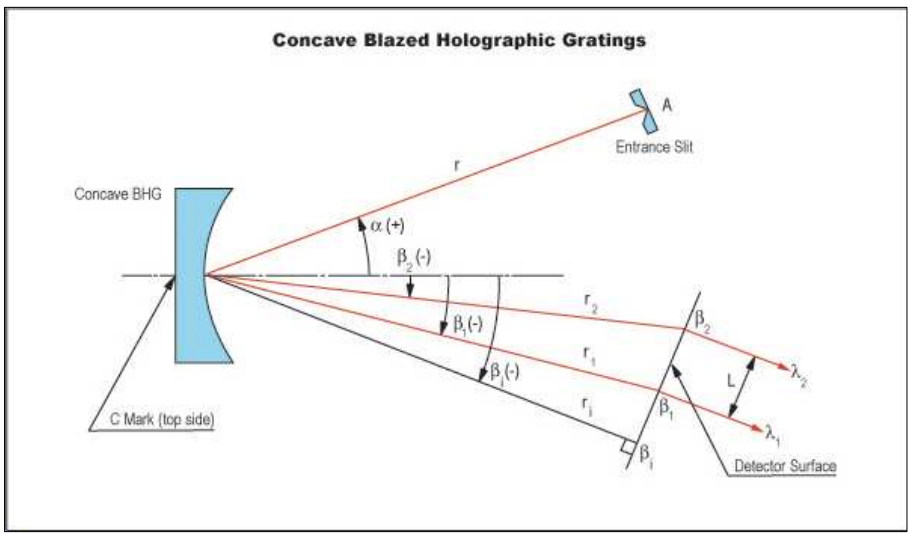


Fig. 63 Various factors of concave grating for designing spectrograph

Table 8. Various factors of 523-03-120 grating

| Factors | Values |
|---|---|
| **Diameter** | 48mm |
| **Focal Length** | 89.87mm |
| **La** | 100mm |
| **Lh** | 90.1mm |
| **α (degree)** | -14.144 |
| **βh (degree)** | 48 |
| **Groove density (gr/mm)** | 340 |
| **K** | 1 |

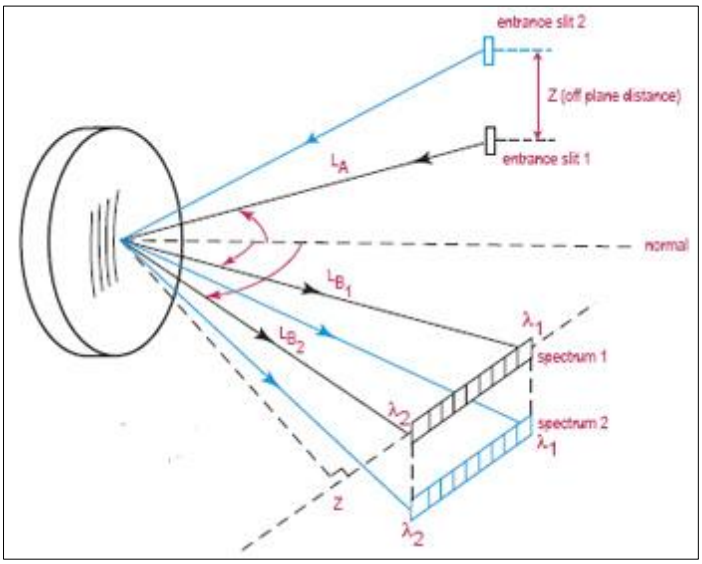


Fig. 64 Dual images formed by a single concave grating using two entrance slits

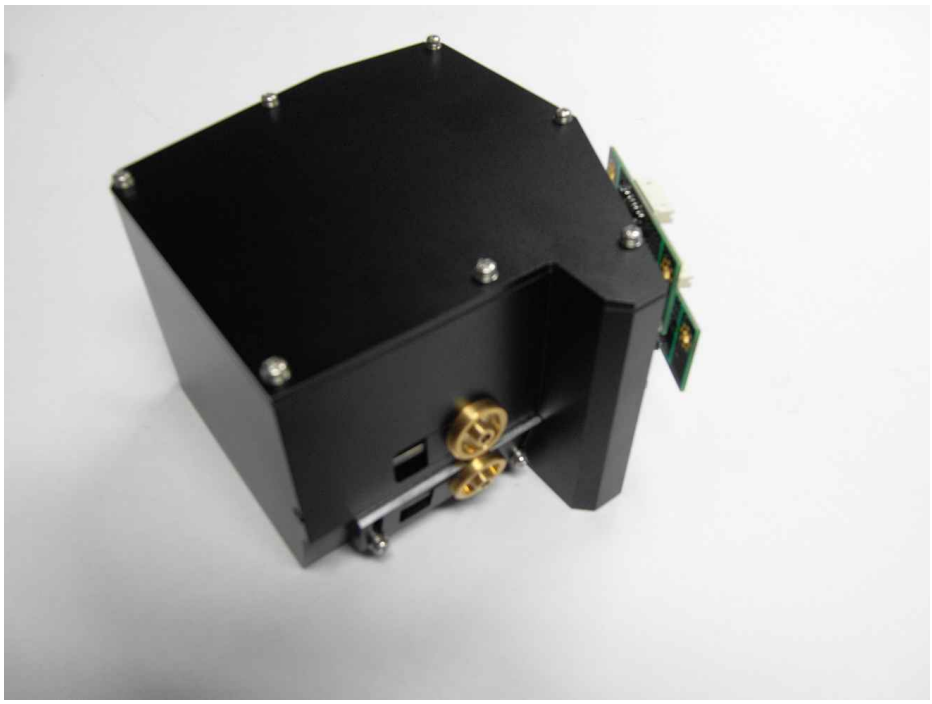

Fig. 65 Fabricated dual image spectrograph with two entrance slits

To detect the dispersed light, two linear image CCD sensors were employed. As shown in Fig. 66, the model of CCD was TCD1304DG produced by Toshiba. This model is commonly used for the detector of a bar code scanner or line camera. It has 3648 pixels and covers from 200 to 1000nm. Normally, CCD needs to be cooled using TEC electric cooler because the dark noise is related with temperature. But in this study, to remove the noise, buffering circuit and signal averaging by software were applied not to use the temperature controller. The buffering circuit is shown in Fig. 67. The AD converting chip used in this fabrication is AD 7667.

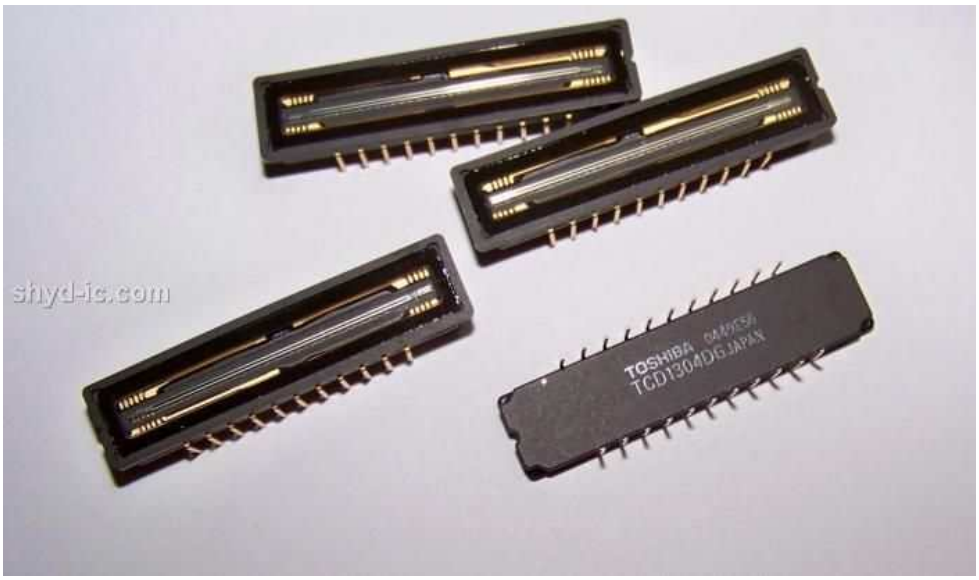


Fig. 66 CCD linear image sensor (TCD1304DG) used in spectrograph

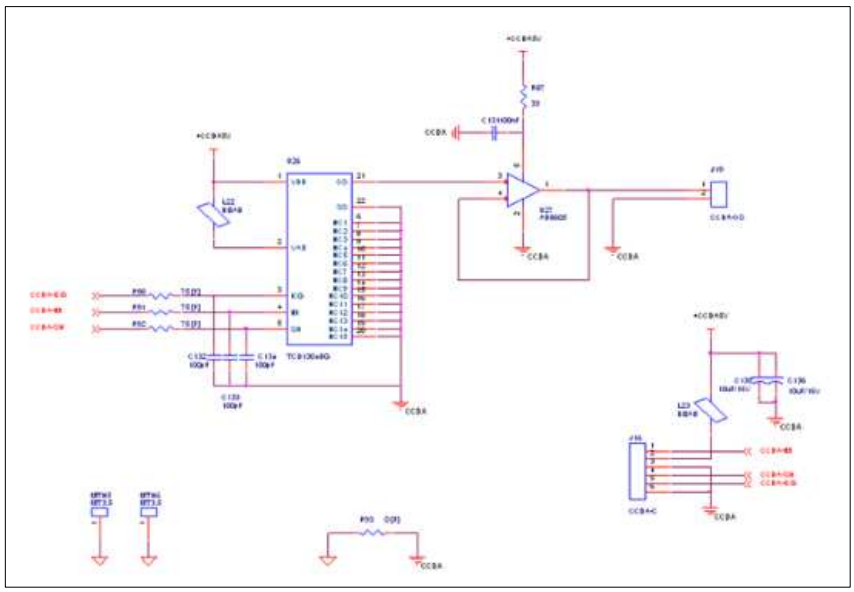

Fig. 67 Buffering circuit of removing CCD noise

## 2.4 Software

Windows based application software was also developed using Visual C++ and Visual Basic 6.0. Visual C++ is used for development of low level communication driver and Visual Basic is used for graphic user interface (GUI) and various analysis. Fig. 68 shows the main window of software of measuring absorbance and fluorescence intensity.

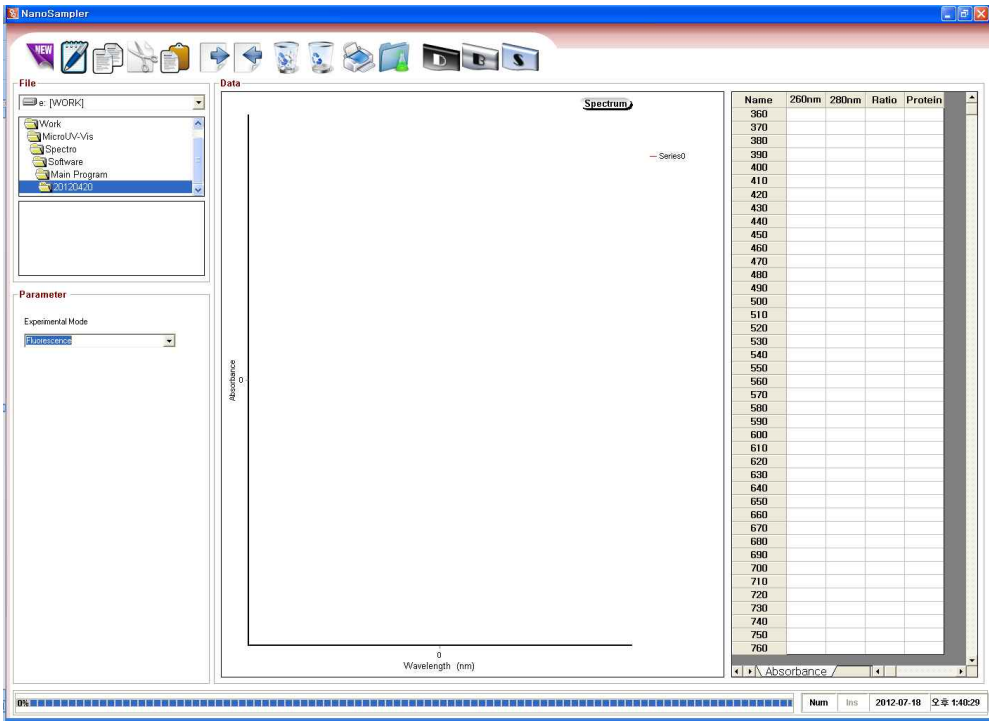


Fig. 68. GUI of software for acquiring the spectrum

## 2.5 System Integration

After designing each part of the system, 3D modeling for system integration was performed using Solid Works 2011. After modeling, 2D drawings were written by Auto-CAD 2005.

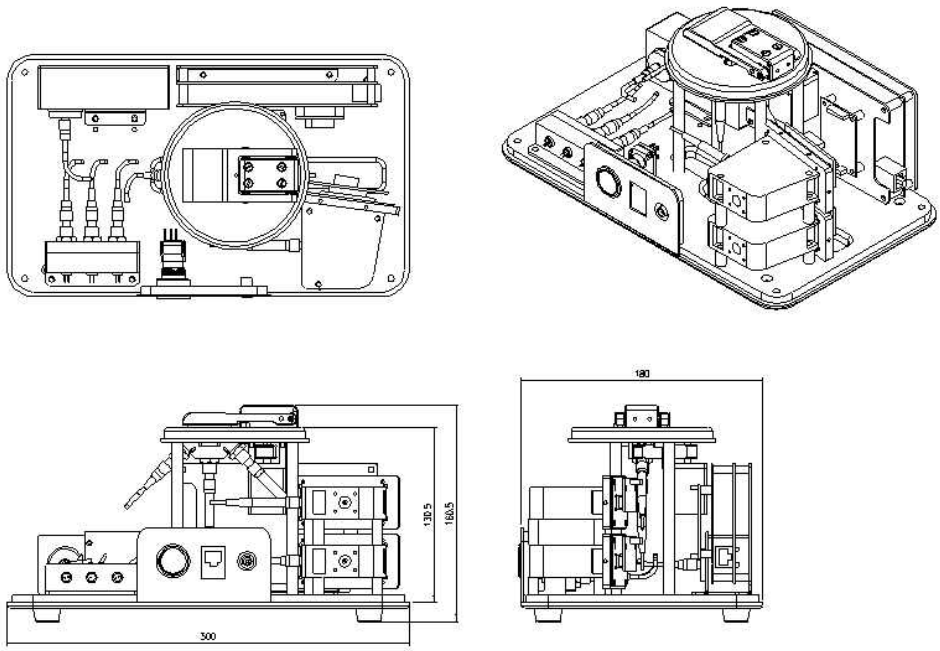


Fig. 69. 2D drawings of total system using Auto-CAD 2005

Fig. 70 shows the 3D modeling of internal parts assembled. And Fig. 71 shows the inside of developed prototype.

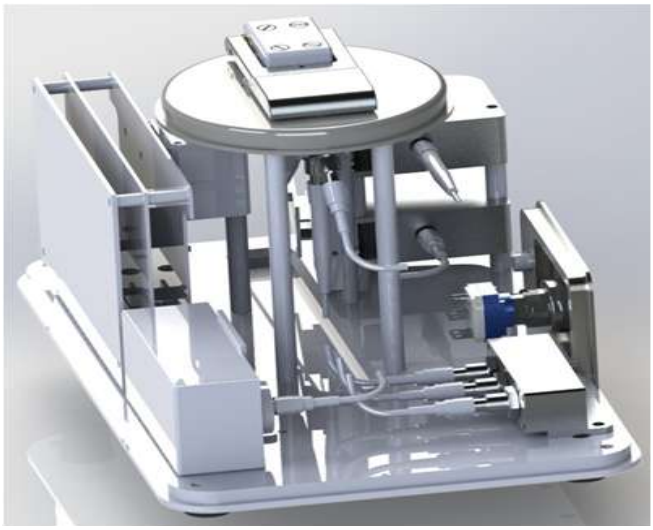

Fig. 70. 3D modeling using the Solid Works 2006

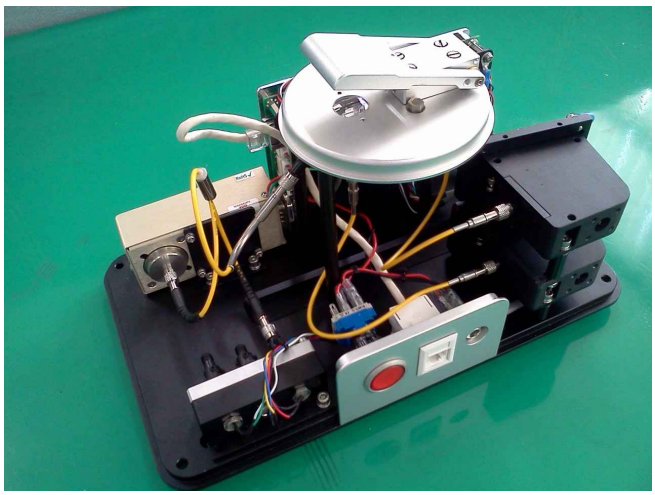

Fig. 71. Inside view of the fabricated prototype

Fig. 72. Total system of prototype closed with case

Fig. 73. The view of the prototype of which the lid was open for attaching the micro-volume sample

For easy drop of the sample on the surface of prism, polymer film was attached on the prism. Using the pippett, sample could be dropped on the prism and fixed successfully as shown in Fig. 74.

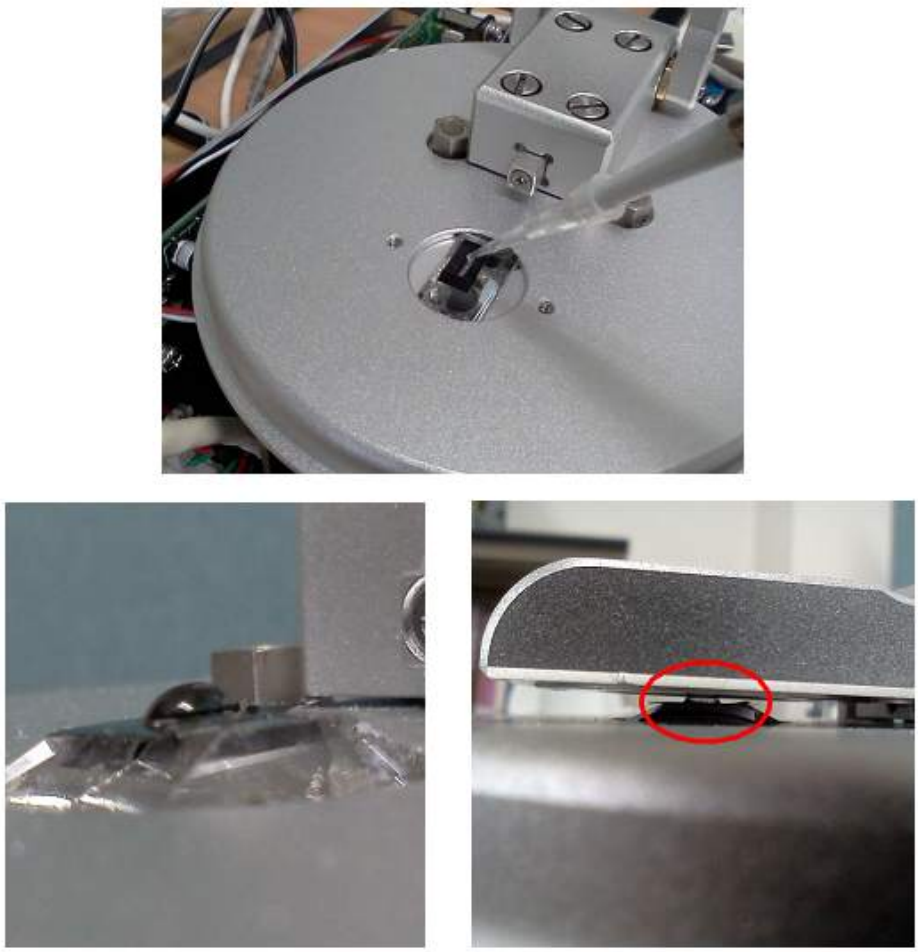

Fig. 74 Dropping and fixing the sample in the designed optics module

## 3. System Evaluation

The developed spectrophotometer of this study must preferably be evaluated using certified standard rules such as ASTM or USP. But most of the rules were defined for using the conventional spectrometers and it was not appropriate to carry out the performance test of the developed system following the existing rules because of the different features of optics design. Therefore, performance test should be done by the comparison the measurement results of the developed system and existing systems. In this test, NanoDrop 2000 was used for comparing as it is mainly used in field. Table 9 shows the specifications of Nano Drop 2000 by Thermo Scientific

Table 9. The specifications of existing system (Nano Drop 2000, Thermo Scientific Instrument, USA)

| **Items** | **Specifications** |
|---|---|
| Minimum Sample Size | 0.5 $\mu\ell$ |
| Path Length | 1 mm |
| Light Source(s) | Xenon flash lamp |
| Detector Type | 2048 - element linear silicon CCD array |
| Wavelength Range | 190 - 840 nm |
| Wavelength Accuracy | 1 nm |
| Spectral Resolution | $\leq$ 1.8 nm |
| Absorbance Accuracy | 3% (at 0.74 at 350 nm) |
| Detection Limit | 2 $ng/\mu\ell$(dsDNA) |
| Baseline Noise | 0.002 AU |

In addition to the listed on the specifications of current existed system, linearity, base line noise and absorbance sensitivity, fluorescence sensitivity should also be tested. Baseline noise is an indicator for checking the stability of the optics design. The target performance of the system developed is presented as shown in Table 10.

Table 10. The target specifications of development in this study

| **Items** | **Target of development** | **Existing system** |
|---|---|---|
| Minimum Sample Size | 0.2 $\mu\ell$ | 0.5 $\mu\ell$ |
| Maximum Path Length | 2.8 mm | 1mm |
| Wavelength Range | 190 - 900 nm | 190 - 840 nm |
| Wavelength Accuracy | 1 nm | 1 nm |
| Spectral Resolution | $\leq$ 1.8 nm | $\leq$ 1.8 nm |
| Absorbance Accuracy | < 3% with Nano-Drop | < 3% |
| Detection Limit | 2 $ng/\mu\ell$(dsDNA) | 2 $ng/\mu\ell$ (dsDNA) |
| Baseline Noise | 0.001 AU | 0.002 AU |

### 3.1 Materials and Method

In previous experiment, the path length was determined as 2.81mm when the sample height is 1mm and the minimum sample volume was 0.2 $u\ell$ when the sample height is 0.1 mm.

Wavelength range can be defined by the mechanical wavelength range or by the actual wavelength range. In the mechanical wavelength range, the minium and maximum wavelength can be determined by mathematical wavelength calibration. And actual wavelength range can be determined by real measurement of light source or by measurement of light intensity transmitted through distilled water placed between the prism and window.

To calibrate the wavelength on each pixel of CCD detector, standard lamp can be used. Standard lamp for wavelength calibration was NIST certified Hg-Ar lamp from Ocean Optics. Fig. 75 shows the numbers of peaks of light emitted from the light source. Theoretically the relation between wavelength and CCD pixel follows 3rd or 2nd order regression curve as shown on formula 17 because the wavelength interval of dispersed light is not regular for whole wavelength range as shown in Fig. 76.

$$\lambda(channel) = A \times channel^3 + B \times channel^2 + C \times channel + D \quad \text{----------(17)}$$

where,

$\lambda(channel)$ : wavelength on each channel of CCD

$A, B, C, D$ : variables and constant

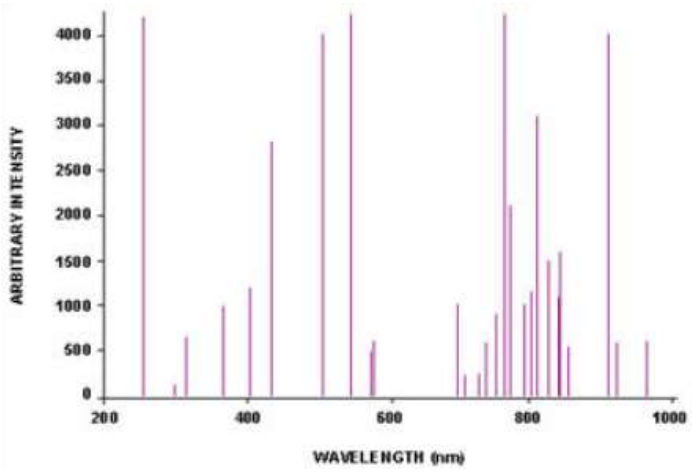


Fig. 75 Various specific peaks by atomic radiation of Hg-Ar lamp

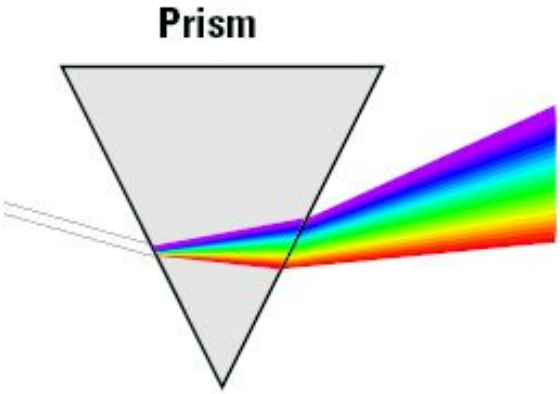


Fig. 76 Different wavelength interval by the different refractive angle

Wavelength accuracy could be tested by checking the unique peak at 656.1nm of deuterium lamp. And the other way is comparing the data measured of same with Nano-Drop. For this test, 23ng/nℓ Calf-Thymus DNA was measured using

Nano-Drop and developed system.

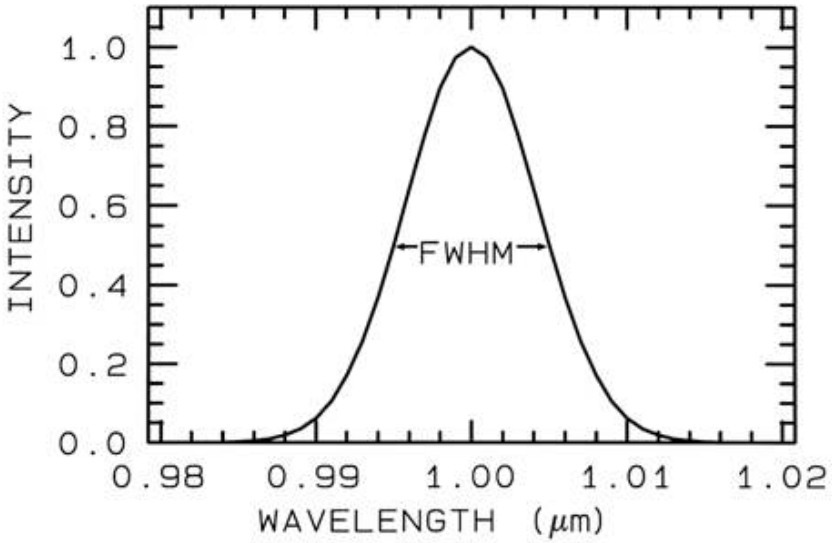


Fig. 77 FWHM of spectrum represents the wavelength resolution of the absorption and fluorescence spectrum

Wavelength resolution can be determined by full width half maximum (FWHM) of Hg atomic line spectrum as shown in Fig. 77. Wavelength resolution is very important in absorbance accuracy. If resolution is poor, the peaks can be over-layed and the correlation between concentration and absorbance does not follow Beer-Lambert's law.

Absorbance accuracy, repeatability, sensitivity and LOD was tested by measuring samples in different concentrations. To perform this, Calf Thymus DNA samples of 100 $ng/u\ell$ and 1000 $ng/u\ell$ were measured by developed system and Nano-Drop 2000.

To test the linearity, R value of calibration curve of quantification can be

thought as indicator.

Base line noise test was peformed by calculating signal to noise of base wavelength after measuring distilled water for ten times.

Finally, fluorescence detection limit was tested following the ASTM method. In this test, PicoGreen DNA of 0.1 pmol was measured to determine of fluorescence LOD.

## 3.2 Results and Discussion

### 3.2.1 Wavelength Range

To calibrate the wavelength to match dispersed light to the pixels of CCD, the regression curve was generated as shown in Fig. 78 and wavelength values on each pixels are listed on Table 11. From this calibration result, mechanical wavelength range was determined from 186.62 to 1030.69 nm

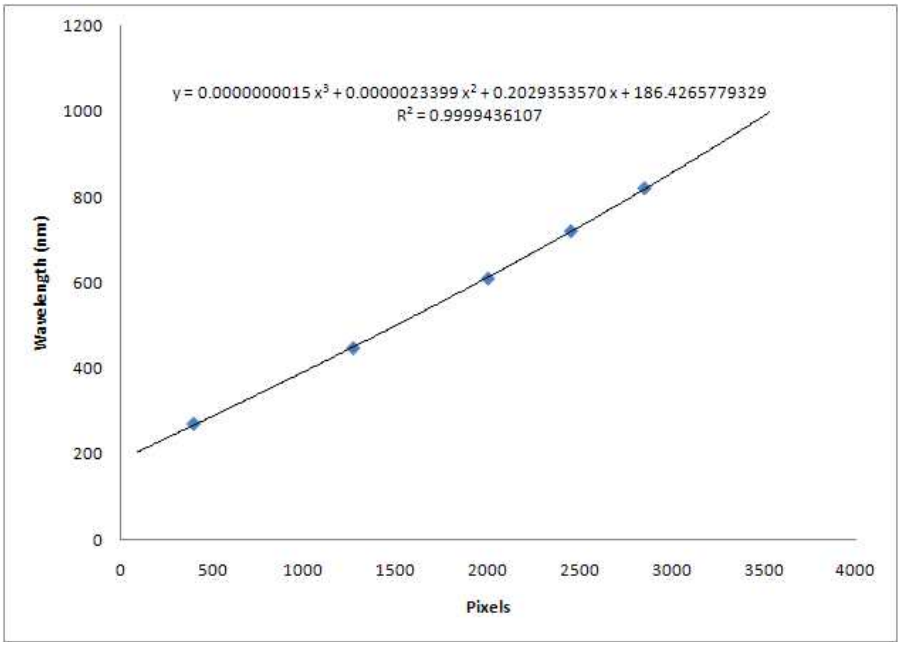


Fig. 78 Wavelength calibration curve between the wavelength and CCD pixels

Table 11. Wavelength determined on each pixel

| Pixel | Wavelength |
|---|---|
| 1 | 186.6295 |
| 500 | 288.6667 |
| 1000 | 393.2018 |
| 1500 | 501.1569 |
| 2000 | 613.6569 |
| 2500 | 731.8268 |
| 3000 | 856.7917 |
| 3648 | 1030.695 |

To define the active wavelength range, standard D2 lamp was measured by connecting it to the spectrograph directly. Fig. 79 shows the spectrum of D2 lamp measured using the developed spectrograph. From this data, actual start wavelength is 205nm.

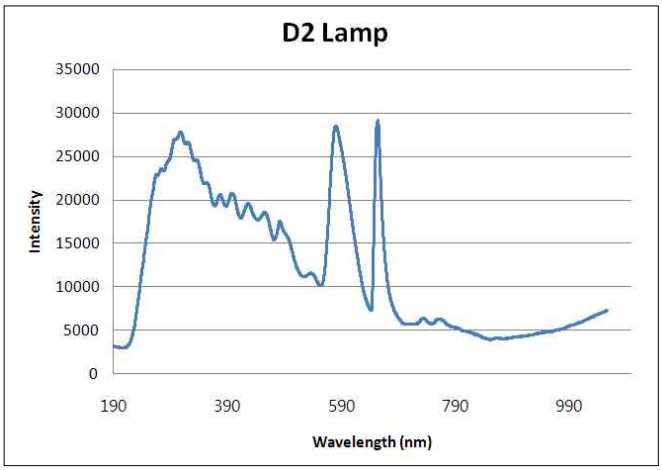


Fig. 79 Light intensity profile of D2 lamp measured by developed spectrograph in this study

The another method to check the actual wavelength range is the measurement of distilled water and the result data is shown in Fig. 80. In this spectrum, the wavelength starts from also 205nm similar to the result of the D2 measurement.

In summary, the results show that mechanical wavelength range is 186nm to 1030nm and actual wavelength range is 205nm to 1030nm.

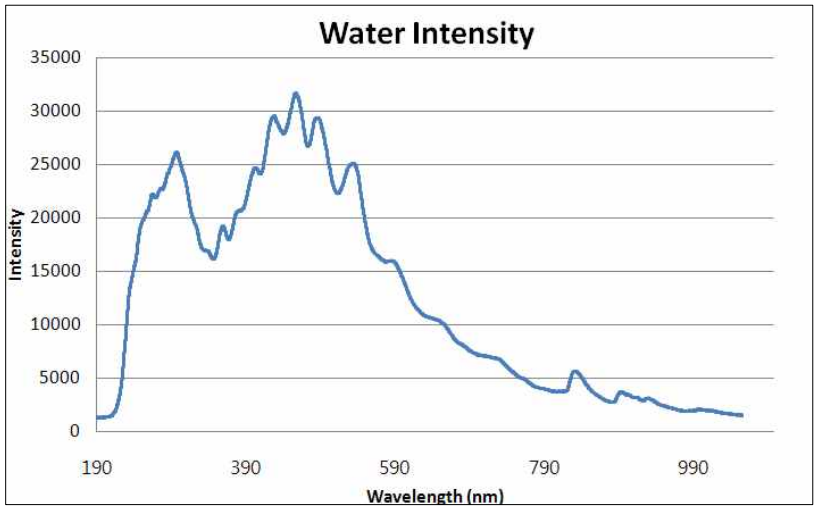


Fig. 80 Intensity profile of transmitted light via distilled water measured by developed system

### 3.2.2 Wavelength Accuracy

The light intensity spectrum of the standard D2 lamp was measured by developed system. From this spectrum, the wavelength of D2 line was 655.7nm and 0.4nm far from standard value of 656.1nm

23ng/nℓ Calf-Thymus DNA in TE buffer was measured by developed system and Nano-Drop. The peak wavelength of the spectrum was 260nm in Nano-Drop

and 260.5nm in developed system. From these results, the wavelength accuracy was determined to be 0.5nm.

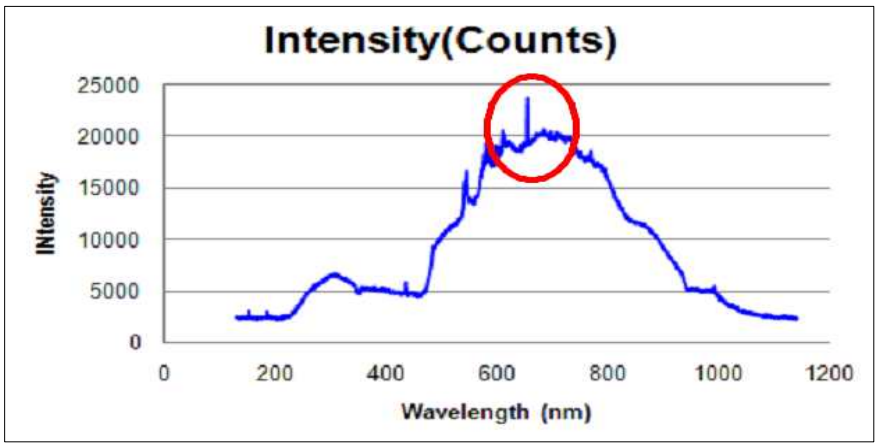


Fig. 81 The specific peak (656.1nm)of D2 lamp in the intensity spectrum measured by developed prototype

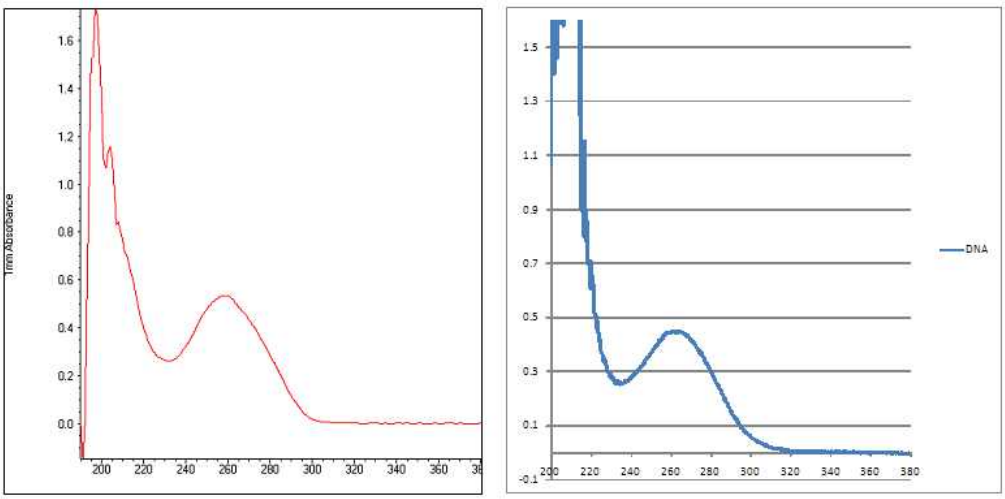


Fig. 82 The spectrum of Calf-Thymus DNA measured by NanoDrop (left) and the developed system (right)

### 3.2.3 Wavelength Resolution

FWHM was determined by measuring Hg-Ar lamp. As shown in Fig 83, the spectrum around 250nm was saturated because of the too strong energy and the peak of 312nm was used for calculating the FWHM. The calculation result was 1.7nm slightly smaller than target value of 1.8nm.

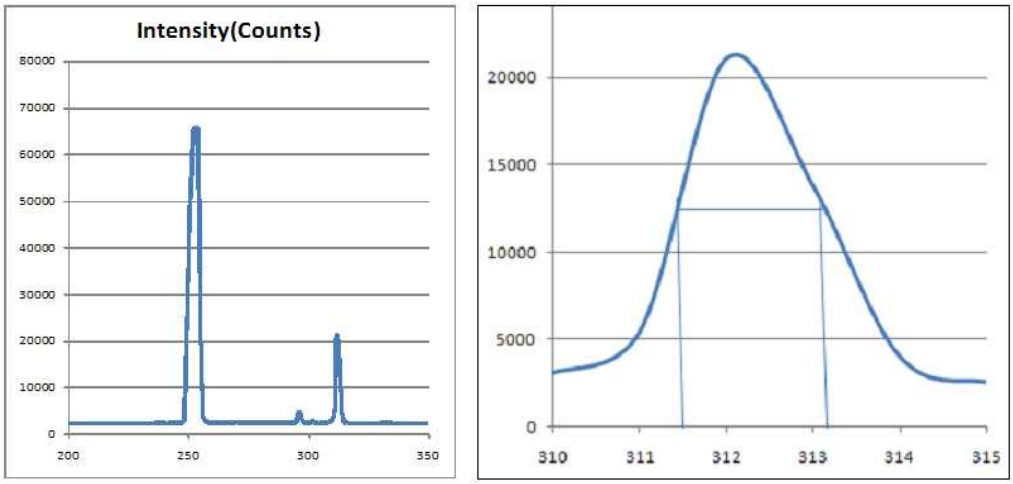


Fig. 83 Spectrum of Hg-Ar lamp measured by developed system

### 3.2.4 Baseline Stability

Baseline stability can be defined by the standard deviation of 10 times measurement of distilled water. Normally water is used as the solvent for DNA and it can be thought as a material for the measurement of baseline. Fig. 84 and 85 show the baseline noise test results by developed system and existing system. The results were 0.0012AU and 0.002AU in standard deviation. As a result of noise test, it is proved that the developed system has a better performance of noise.

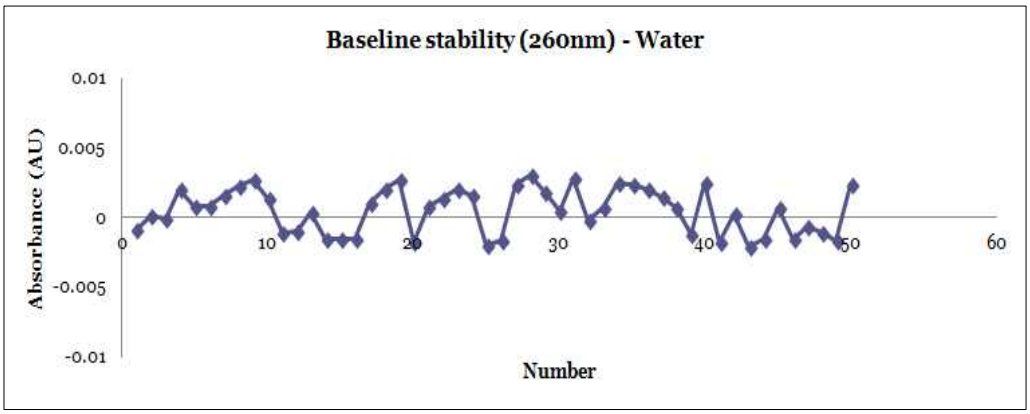


Fig. 84 Repetitive absorbance measurement result of distilled water by developed system

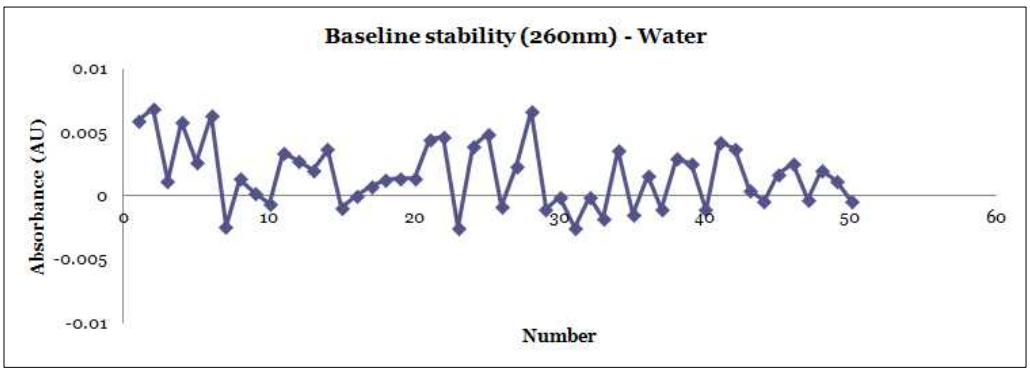


Fig. 85 Repetitive absorbance measurement result of distilled water by existing system

### 3.2.5 Absorbance Accuracy and Repeatability

Absorbance repeatability is another indicator to check the stability of system. To determine absorbance repeatability, CV (coefficient of variation) should be used because the simple standard deviation of measurements can be varied as

absorbance can be varied by changing the optical path length. CV can eliminate the effect of sample concentration by calculation of the standard deviation over average of data.

In this experiment, samples of 100 $ng/u\ell$ , 1000 $ng/u\ell$ were measured for 10 times by developed system and NanoDrop2000. And path length was fixed to 0.5mm for developed system and sample volume was 2.5 $u\ell$.

Table 13 and 14 show the experimental results for 100 $ng/u\ell$ and 1000 $ng/u\ell$. In these results, absorbance level was different for same concentration as the final data from Nano-Drop 2000 was internally multiplied by some factor. Considering the result of CV, the repeatability was enhanced in developed system. It can be thought that the mechanical stability was enhanced by fixing the optical components and longer path length. If the absorbance of developed system would be multiplied by 20, the average absorbance at 260nm is 2.052 and the gap from the Nano-Drop 2000 is about 2.8%.

Table 12 Absorbance repeatability test results at 100 $ng/u\ell$ by developed system and NanoDrop 2000

| | Developed System | | NanoDrop 2000 | |
|---|---|---|---|---|
| No. | AU(260nm) | AU(280) | AU(260nm) | AU(280) |
| 1 | 0.1023 | 0.0542 | 1.998 | 1.054 |
| 2 | 0.1025 | 0.055 | 1.995 | 1.041 |
| 3 | 0.1024 | 0.0544 | 1.993 | 1.048 |
| 4 | 0.1027 | 0.055 | 1.988 | 1.05 |
| 5 | 0.1029 | 0.0548 | 1.985 | 1.052 |
| 6 | 0.1029 | 0.0552 | 1.985 | 1.044 |

| | | | | |
|---|---|---|---|---|
| 7 | 0.1026 | 0.0546 | 1.985 | 1.05 |
| 8 | 0.1023 | 0.0541 | 1.986 | 1.046 |
| 9 | 0.1028 | 0.0548 | 2.004 | 1.058 |
| 10 | 0.1025 | 0.0548 | 2.003 | 1.066 |
| STD | 0.000228 | 0.00036 | 0.007199 | 0.007 |
| AVG | 0.1026 | 0.0547 | 1.9926 | 1.0509 |
| CV | 0.0022 | 0.0065 | 0.0036 | 0.0068 |

Table 13 Absorbance repeatability test results at 1000 $ng/u\ell$ by developed system and NanoDrop 2000

| | Developed System | | NanoDrop 2000 | |
|---|---|---|---|---|
| No. | AU(260nm) | AU(280) | AU(260nm) | AU(280) |
| 1 | 1.0685 | 0.5753 | 20.577 | 11.107 |
| 2 | 1.0685 | 0.5734 | 20.653 | 11.113 |
| 3 | 1.0698 | 0.5755 | 20.46 | 10.924 |
| 4 | 1.0628 | 0.5716 | 20.615 | 11.028 |
| 5 | 1.0674 | 0.5762 | 20.711 | 11.056 |
| 6 | 1.0647 | 0.5736 | 20.649 | 11.114 |
| 7 | 1.0681 | 0.5739 | 20.751 | 10.962 |
| 8 | 1.0689 | 0.5757 | - | - |
| 9 | 1.0693 | 0.5739 | 20.567 | 10.907 |
| 10 | 1.0717 | 0.5744 | 20.823 | 11.138 |
| STD | 0.0025 | 0.0013 | 0.1079 | 0.0088 |
| AVG | 1.0680 | 0.5744 | 20.6451 | 11.0388 |
| CV | 0.0023 | 0.0023 | 0.0052 | 0.0080 |

### 3.2.6 Absorbance Sensitivity and LOD

From the 3.2.5, the calibration curves of developed system and Nano-Drop 2000 were determined. In this results, the slope of calibration curve was 0.0207 for developed system and 0.0209 for Nano-Drop 2000. And each standard deviation (CV) results were 0.0022, 0.0036 at 100 $ng/u\ell$ and 0.0023, 0.0052 at 1000 $ng/u\ell$. From these results, the sensitivity was enhanced as listed in Table 14.

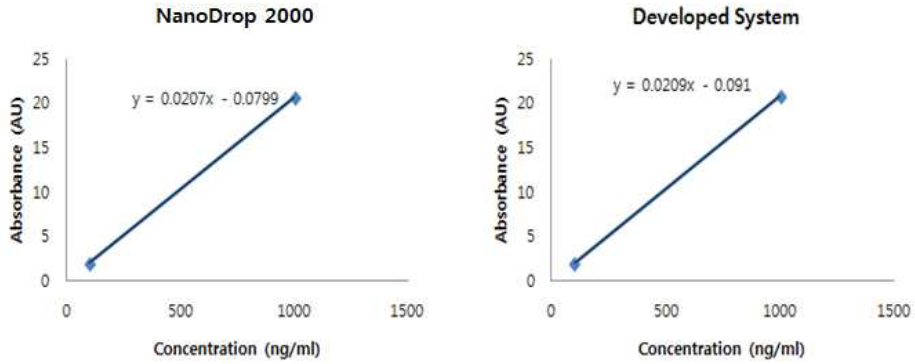


Fig. 86 Calibration curves between the absorbance and sample concentration of each system

Table 14 Sensitivity results at 100 $ng/u\ell$ and 1000$ng/u\ell$ by developed system and NanoDrop 2000

| | 100$ng/u\ell$ | | 1000$ng/u\ell$ | |
|---|---|---|---|---|
| | NanoDrop 2000 | Developed System | NanoDrop 2000 | Developed System |
| Slope | 0.0207 | 0.0209 | 0.0207 | 0.0209 |
| Noise (CV) | 0.0036 | 0.0022 | 0.0052 | 0.0023 |
| Sensitivity | 5.75 | 9.50 | 3.98 | 9.09 |

Table 15 LOD results by developed system and NanoDrop 2000

| | NanoDrop 2000 | Developed System |
|---|---|---|
| Absorbance (AVG) – 10mm equivalent | 1.993 | 2.001 |
| RMS Noise (Baseline) | 0.0028 | 0.0012 |
| LOD | 0.422 ng/ul | 0.18ng/ul |

### 3.2.7 Linearity

Correlation between concentration and absorbance was determined by measuring various concentrations of samples and calculated R value was used to evaluate the linearity and detection limit of the developed system.

In this experiment, samples of 100ng/$\mu\ell$, 300ng/$\mu\ell$, 600ng/$\mu\ell$ and 1000 ng/$\mu\ell$ were measured to make calibration curve. In quantification calibration, R value was 0.9993.

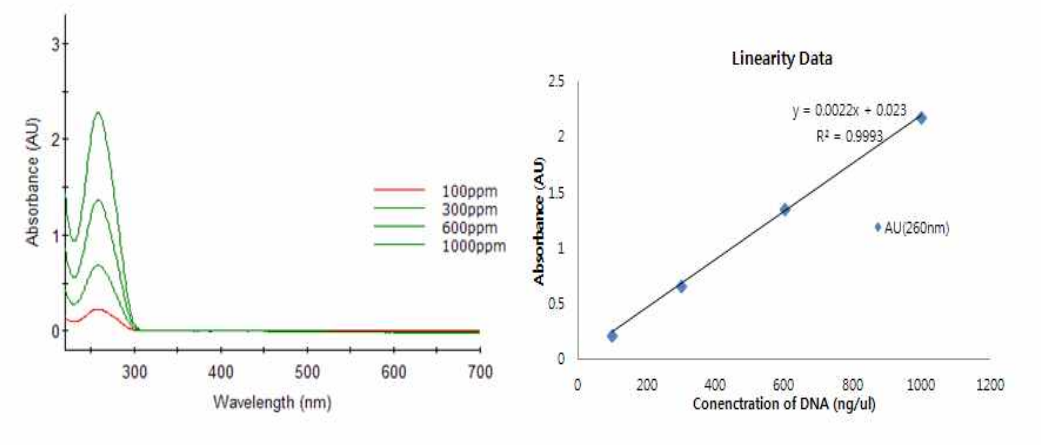


Fig. 87 Absorption spectra of various concentration and regression curve between absorbance and concentration achieved by the developed system

### 3.2.8 Fluorescence LOD

In ASTM E579-04, LOD of Fluorescence is defined by the formula 18. Originally in this method, Quinine sulfate should be measured to calculate the LOD. But in this experiment, Qauant-iT$^{TM}$ PicoGreen with dsDNA Reagent Kit was used because the developed system in this study should be used for biological sample such as DNA and proteins. The sample was made by 30 $\mu\ell$ Lambda DNA of 0.1 p mol, 5 $\mu\ell$ Picogreen dye and 950 $\mu\ell$ buffer. Thus, the concentration of DNA in buffer was 102 p M.

$$LOD\ (mol) = (C / S) \times (N \times 3) \quad \text{----------(18)}$$

where,

$C$ : sample concentration

$S$ : fluorescence intensity

$N$ : RMS noise of baseline

In Fig. 88, the left spectrum peak is by Ray-leigh scattering of light source and the second peak is the fluorescence spectrum. In this spectrum, fluorescence intensity height was about 5,000. As listed on the Table 16, baseline noise at 700nm about 15 in standard deviation. From this result, the LOD of fluorescence for DNA is 0.9 f mol (918 f M in concentration )

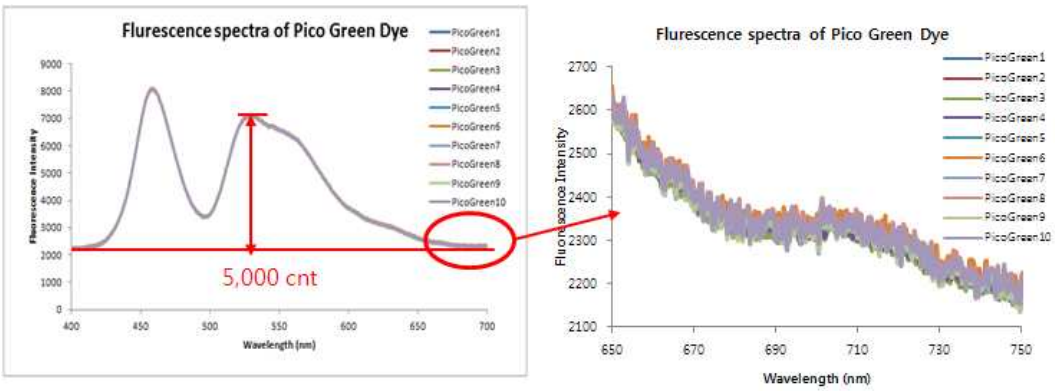


Fig. 88 Fluorescence spectra of pico-green DNA measured by the developed system

Table 16 Baseline results for 10 measurements of Qauant-iT™ PicoGreen with dsDNA

| No. | Baseline Intensity |
|---|---|
| 1 | 2308 |
| 2 | 2308 |
| 3 | 2323 |
| 4 | 2315 |
| 5 | 2330 |
| 6 | 2336 |
| 7 | 2336 |
| 8 | 2297 |
| 9 | 2311 |
| 10 | 2297 |
| STDEV | 15 |

## 4. Conclusion

Spectrophotometer based on new optics design using total internal reflection was developed for simultaneous measurement of fluorescence and absorption spectra of small nucleic acid samples.

The developed system was also evaluated by measuring spectra of various samples and comparing with that of NanoDrop 2000. Target specifications were determined by reviewing the performance list of the existing instrument.

As listed in Table 17. the performances of absorbance of new developed system were relatively enhanced comparing those of NanoDrop 2000 by enlarging the path length and by enhanced optical stability without moving the optical components. For the fluorescence LOD, the result of developed system is similar to that of the NanoDrop 3000 fluorescence spectrometer.

Table 17. Test results of the developed system and NanoDrop units.

| Items | Test Result | NanoDrop 2000 (UV-Vis spectrometer) |
|---|---|---|
| Minimum Sample Size | 0.2 $u\ell$ | 0.5 $u\ell$ |
| Maximum Path Length | 2.8mm | 1mm |
| Wavelength Range | 186-1030 nm | 190 - 840 nm |
| Wavelength Accuracy | 0.5 nm | 1 nm |
| Spectral Resolution | 1.7nm | $\leq$ 1.8 nm |
| Absorbance Accuracy | 2.8% | < 3% |
| Absorbance Detection Limit | 0.18 $ng/u\ell$ (dsDNA) | 0.422 $ng/u\ell$ (dsDNA) |
| Baseline Noise | 0.0012AU | 0.0028AU |
| Absorbance Repeatability (CV) | 0.00228 (100$ng/u\ell$) | 0.0036 (100$ng/u\ell$) |
| Absorbance Sensitivity | 9.5 | 5.75 |
| `Fluorescence Detection Limit (mol) | 0.9 fmol DNA | 1 fmol fluorescein (NanoDrop 3000 Fluorescence spectrometer) |

# Ⅴ. Overall Conclusion

The objective of this study is to develop a spectrophotometer for fluorescence and absorbance measurements of micro volume nucleic acids to get the higher sensitivity, stability and flexibility comparing existing spectrophotometers for micro-volume nucleic acids of bio samples.

In order to fulfill the objectives of this study, new concept of optics using a prism and a window was presented and the detailed optics design and geometry were determined based on Snell's law and Fresnel's law. And optical simulation was performed using TracPro 6.0 to analyze the optical dimensions and predict minimum sample size in various sample heights.

To evaluate the design of optics, primary experimental device was fabricated and several data were compared with those of conventional UV-Vis spectrometers. As a result, it was proved that the optics were correctly designed by confirming expected path length and experimental path length were very close. And also minimal sample volume could be reached to 0.2 $u\ell$ in 0.1mm sample height condition.

Using the designed optics, a dedicated spectrophotometer was developed to measure absorption and fluorescence spectrum simultaneously for small volume nucleic acids in one system. It was evaluated by measuring Calf-Thymus DNA and PicoGreen-DNA in different concentrations. From the results, enlarging the beam path length and fixing the optical components enabled the system to get the enhancement in sensitivity, LOD, baseline stability. And it also improved the flexibility to researchers by measuring absorption and fluorescence spectrum in one system without changing the optical geometry.

Fluorescence measurement techniques of nucleic acids has been rapidly

developed and the usage of fluorescence spectrometer for small size sample will be more increased. In this case, the developed integrated system in this study will be a good solution to cover both traditional and new experimental method.

# Ⅵ. Future Works

A spectrophotometer which measures fluorescence and absorbance of micro volume nucleic acids simultaneously with high sensitivity, stability and flexibility is developed. However, there are several things to improve for commercializing the spectrophotometer.

Firstly, the strength of material of window used for total internal reflection should be greater than that of this study. Because it's thickness should be just 0.2mm which could be easily broken when cleaning the window. In this study, fused silica cover slip was used to enhance the transparency of UV light but the other materials such as a sapphire can be employed to protect a window from external damage.

Secondly, the multi-plex optical fiber module must be more finely fabricated for the cores of each fiber to be aligned to the center of the beams. In this study, three cores are linearly positioned and the xenon light source is placed on the center of cores for accurate measurement of absorbance. However, in this case, LEDs can't be focused to the center of the sample and fluorescence intensity could be weaker than expected. To enhance the fluorescence intensity, the technique of multi-plex of the optical fiber should be enhanced.

Finally, the spectrophotometer needs to measure multi-samples in one time for the fast measurement. This study was focused to the enhancement of sensitivity and hybridization by measurement both absorbance and fluorescence for one sample. However, in field of diagnostics, there are lots of samples to be measured and the well plate or sample changer could be very strong tool for the multi-sampling.

# Ⅶ. References


1. Agilent Technologies. 2000. Fundamentals of UV-visible spectroscopy. Agilent Technologies.

2. Axelrod, D. 2001 Total Internal Reflection Fluorescence Microscopy in Cell Biology. Traffic 2 (2001) 764-774

3. ASTM Standards. 2004. E 579-04 : Standard Test Method for Limit of Detection of Fluorescence of Quinine Sulfate in Solution.

4. Blumenthal, A., L. Kuznetzova, O. Edelbaum, V. Raskin, M. Levy and I. Sela. 1999. Measurement of green fluorescence protein in plants: quantification, correlation to expression, rapid screening and differential gene expression. Plant Science 142 (1999) 93-99.

5. Held, P. 2001. Nucleic Acid Purity Assesment Using A260/A280 Ratios. Available at http://www.biotek.com/resources/articles/nucleic-acid-purity-a260a280.html

6. Boyer, R. F. 2000. Modern Experimental Biochemistry. 3rd ed. Prentice-Hall

7. Bruns, D. E., R. Edward and A. Carl. 2007. Fundamentals of molecular diagnostics. Elsevier. pp. 31-117

8. Bustin, S. A. 2004. A-Z of quantitative PCR. La Jolla, CA 92038-2525, USA, International University Line.

9. Crisp, J. and B. Elliott. 2005. Introduction to fiber optics. 3rd ed. Newnes. Linacre House, Jordan Hill, Oxford OX2 8DP 30 Corporate Drive, Burlington, MA 01803

10. Dzagli, M. M., V. Canpean., M. Iosin, M. A. Mohou and S. Astilean. 2010. Study of

the interaction between CdSe/Zns core-shell quantum dots and bovine serum albuimin by spectroscopic techniques. Journal of Photochemistry and Photobiology A: Chemistry, 215 (2010) 118-122.

11. Generalova, A. N., A. Vladmir, S. Alyona, V. Bikhail, P. Vitaly, and N. Igor. 2012. Quantum dot-containing polymer particles with thermosensitive fluorescence. Biosensors and Bioelectronics 39 (2012) 187-193.

12. Georgescu, V., M. Voulborn. 2002. Nanobiotechnologie als Wirtschaftskraft, Campus Verlag GmbH, Frankfurt am Main (In Korean)

13. Gotze, S and R. Saborowski. 2011. NanoDrop fluorometry adopted for microassays of proteasomal enzyme activities. Analytical Biochemistry 413 (2011) 203-205

14. Grundmann, M. and F. M. Matysik. 2012. Analyzing small samples with high efficiency : capillary batch injection-capillary eletrophorosys-mass spectroscopy. Anal Bioanal Chem, 404 (2012) 1713-1721

15. Jenkins, F. A. and H. E. White. 2001. Fundamentals of Optics. 4th ed. McGraw-Hill. pp.523-543

16. Kang, W., S. J. Bae and G. V. Papayan. 2007. Method for measuring bio-chip using regular total internal reflection light source. KR Patent No. 10-0768038

17. Kochi, S., H. Niederstatter and W. Parson. 2005. DNA extraction and quantitation of forensic samples using the phenol-chloroform method and real-time PCR. Methods in Molecular Biology, 297 (2005) 13-30.

18. Kim, D. S., Y. T. Jeong, H. J. Park, J. K. Shin, P. Choi, J. H, Lee and G. B. Lee. 2003. An FET-type charge sensor for highly sensitive detection of DNA sequence.

Biosensors and Bioelectronics, 20 (2003) 69-74

19. Kim et al. 2008. Food science dictionary. Kwang-il. (In Korean)

20. Lakowicz, J. R. 1999. Principles of Fluorescence Spectroscopy. 2nd ed. Kluwer Academic / Plenum Publishers

21. Loewen, E. G and E. Popov. 1997. Diffraction gratings and application. Marcel Dekker, Inc. 270 Madison Avenue, New York, New York 10016

22. Liu, R. H., J. Yang, R. Lenigk, J. Bonanno and Grodzinski P. 2004. Self-Contained, Fully Integrated Biochip for Sample Preparation, Polymerase Chain Reaction Amplification, and DNA Microarray Detection. Analytical Chemistry 76 (2004) 1824 - 1831

23. Marras, S. A. E. and J. Hansen. 2008. Molecular Becon Probes: Micro-Volume Fluorescence Measurement of HPLC Isolated Probes. Application Note Rev 4/08. Thermo Fisher Scientific.

24. Morozkin, E. S., P. P. Laktionov, E. Y. Rykova and V. V. Vlassov. 2003. Fluorometric quantification of RNA and DNA in solutions containing both nucleic acids. Analytical Biochemistry, 322 (2003) 48-50.

25. Mortimer-Jones, S. M., M. G. K. Jones, R. A. C. Jones, G. Thompson, G. I. Dwyer. 2009. A single tube, quantitative real-time RT-PCR assay that detects four potato viruses simultaneously. Journal of Virological Methods, 161(2009) 289-296.

26. Nielsen, K., H. S. Mogensen, B. Eriksen, J. Hedman, W. Paron and N. Morling. 2006. Comparison of six DNA quantification methods. International Congress Series, 1288 (2006) 759-761.

27. Olympus. Jablonski Diagram. Microscopy Resource Center. Available at http://www.olympusmicro.com/primer/java/jablonski/jabintro/

28. Park, J. J., W. C. Youn and S. W. Kang. 2011. Photochemistry. Free Academy. pp.2-100 (In Korean)

29. Pecq, J. B. and C. Paoletti. 1966. A new fluorometric method for RNA and DNA determination. Analytical Biochemistry, 17 (1966) 100-107.

30. Phenix Research Products. 2011. Overview of common fluorescent dyes used in Nucleic Acid quantitation. Application Note rev 11.03 (2011)

31. Rengarajan, K., S. M. Crostol, M. Mehta and J. M. Nickerson. 2002. Quantifying DNA concentrations using fluorometry : a comparison of fluorophores. Mol. Vision, 8 (2002) 416-421.

32. Ro, S., C. Park, J. Jin, K. M. Sanders and W. Yan. 2006. A PCR-based method for detection and quantification of small RNAs. Biochemical and Biophysical Research Communications, 351 (2006) 756-763

33. Schmidt, D. M. and J. D. Ernst. 1995. A fluorometric assay for the quantification of RNA in solution with nanogram sensitivity. Analytical Biochemistry, 232 (1995) 144-146.

34. Sim T. S., 2007. Fabrication of a temperature and fluid controllable microchip for small volume protein analysis. PhD diss., Seoul National University, Department of Computer Science and Engineering. (In Korean)

35. Son et al. 19997. Experimental Biochemistry. Tamgudang. pp.313-364 (In Korean)

36. Skoog, D. A., F. J. Holler and S. R. Crouch. 2007. Principles of Instrumental Analysis, 6th ed. Cengage Learning. pp. 313-412 (In Korean)

37. Tang, Y. J., Y. Chen, Z. Chen, T. Xie and Y. Li. 2008, Adsorption of a protein–porphyrin complex at a liquid–liquid interface studied by total internal reflection synchronous fluorescence spectroscopy. Analytica Chimica Acta 614 (2008) 71–76

38. Thermo Fisher Scientific. 2009. 260/280 and 260/230 Ratios. T042-Technical bulletin NanoDrop Spectrometers (2009) Rev 2/09

39. Thompson, N. L. and B. C. Lagerholm, 2005. Total internal reflection fluorescence: applications in cellular biophysics. Current Opinion in Biotechnology, 16 (2005) 13-18

40. TracePro. 2009. TracePro Expert Ver. 6.02. Lambda Research Corporation

41. Walsh, P. S., W. J. Varlaro and R. Reynolds. 1992. A rapid chemiluminescent method for quantitation of human DNA. Nucleic Acids Research, 20 (1992) 5061-5065

42. Warren J. S. 2007. Modern optical engineering. 3rd ed. McGraw-Hill, pp.23-27. (In Korean)

43. Zhang, X., X. Wang and Z. Guanghe. 2008. A one-step real time RT-PCR assay for quantifying rice stripe virus in rice and in the small brown planthopper (Laodelphax strialtellus Fallen). Journal of Virological Methods, 151 (2008) 181-187.

44. Zhang, X., G. Zhou and X. Wang. 2010. Detection of wheat dwarf virus (WDV) in wheat and vector leafhopper(Psammotettix alienus Dahlb.) by real-time PCR. Journal of Virological Methods 169 (2010) 416-419.

# Development of Absorbance and Fluorescence Spectrometer for Micro-Volume Nucleic Acids of Bio-Samples Using Total Internal Reflection

# 내부 전 반사를 이용한 미량 바이오 시료 측정용 흡광 및 형광 분광 광도계의 개발

강 인 성

## 국문 초록

최근 미량 핵산 분석 전용 분광 광도계가 농업, 의학, 생화학, 식품등의 다양한 분야에서 널리 사용되고 있다. 이러한 기기들의 공통적인 특징은 미량의 시료를 측정하기 위해 짧은 광 경로 길이를 가지고 있다는 점과 광 이송 부품을 이동시킨다는 것이다. 이러한 기기적 특징으로 인해 흡광 측정 감도 저하를 가져 올 수 있어 저 농도의 시료를 측정하는 데 있어 기기적 한계를 노출한다. 또한 흡광과 형광 스펙트럼을 동시에 측정하기 위해서는 별도의 장비를 도입해야 하게 되어 높은 비용과 측정의 비효율을 야기하므로 기기의 활용에 있어 사용자의 유연성을 떨어뜨리는 요인이 된다.

본 연구에서는 이러한 단점을 극복하기 위해 프리즘과 윈도우를 사용한 내부 전반사 광학 구조를 제시하여 광경로를 확장함으로써 감도를 높임과 동시에 형광과 흡광을 동시에 측정할 수 있도록 하였다. 광학 치수와 배치의 최적화를 위해 스넬의 굴절 법칙과 프레넬의 반사 법칙에 의해 최적의 입사광 각

도를 결정하였고 TracePro 6.0을 이용한 광학 시뮬레이션을 통해 시료의 용량을 최소화하기 위한 광학 구조 및 시료의 직경과 높이를 최적화하였다. 시뮬레이션 결과 본 광학 시스템의 최대 광 경로는 2.83 mm이며 측정 가능한 최소 용량은 0.09 $u\ell$ 로 결정되었다. 광학 설계를 검증하기 위해 동일한 시료를 기존의 여러 범용 분광 광도계 및 본 연구의 실험 장치를 이용하여 측정한 후 비교하였다. 실험 결과 광 경로의 길이는 설계시의 계산 값과 실험에 의한 계산 값이 각각 2.83 mm, 2.81 mm로 거의 일치하였고, 핵산 시료들의 측정 정확도 역시 기존 분광 광도계와 표준 편차 0.04 이내의 근소한 차이로 일치하여 광학 설계가 적합함을 검증하였다. 또한 최소 용량 실험을 통해 0.2 $u\ell$ 까지 측정 가능함을 보였다.

본 연구에서 설계된 광학 시스템을 기초로 소형화된 형광 및 흡광 스펙트럼을 통합적으로 측정할 수 있는 분광광도계를 개발하였고, 시스템의 성능 평가를 위해 다양한 농도의 Calf-Thymus DNA 와 PicoGreen DNA 시료를 측정하였다. 기존의 바이오 시료 전용 분광 광도계와의 비교를 위해 감도, 측정 한계, 안정성 측면에서 성능 평가를 하였다. 실험 결과, 개발된 시스템과 기존 시스템의 감도는 9.5와 5.75 였으며 검출 한계는 각각 0.18 $ng/ul$ 과 0.42 $ng/ul$ 였다. 또한 바탕선 잡음은 각각 0.0012 AU와 0.0028 AU였다. 형광 측정 감도는 약 0.9 f mol이었다.

이들 실험을 바탕으로 본 연구의 목적인 내부 전반사 광학 설계를 통한 기존 장비 대비 감도의 향상, 안정성의 향상, 유연성 향상이 충족되었음을 확인하였다.

본 연구의 결과를 상용화하기 위해서는 다음의 것들이 기술적으로 개선되어야 한다. 우선, 내부 전반사를 위한 윈도우의 재질의 강도가 세척 과정에서 깨지지 않도록 본 연구에서 사용된 재료보다 더 강해야 한다. 또한 광원들로부터 광을 시료의 정확한 위치로 초점을 맞추기 위해 멀티플렉스 된 광파이

버내의 코어들이 현재보다 중앙으로 정렬되어야 한다. 마지막으로 빠른 측정을 위해 여러 개의 시료를 한꺼번에 측정할 수 있어야 하며 well-plate 및 sample changer와 같은 장치들이 적용될 필요성이 있다.

---

Keywords : 핵산, 분광 광도계, 정량, 핵산 순도, 내부 전반사, 형광, PCR
Student number : 2008-30332